Analytical Methods

ROYAL SOCIETY OF CHEMISTRY

CRITICAL REVIEW

View Article Online
View Journal | View Issue

Cite this: *Anal. Methods*, 2025, **17**, 4300

Cyclodextrin-based architectures for electrochemical sensing: from molecular recognition to functional hybrids

Xingxing Li,[a] Li Fu, *[a] Fei Chen, [a] Yanfei Lv,[a] Rui Zhang,[a] Shichao Zhao [a] and Hassan Karimi-Maleh *[b]

This review surveys recent advances in the integration of cyclodextrins (CDs) with diverse materials for electrochemical detection of a wide range of analytes in environmental, pharmaceutical, and clinical contexts. CDs, featuring a hydrophobic cavity and a hydrophilic exterior, enable selective host–guest binding of small organic and inorganic molecules. By anchoring CDs onto electrode surfaces *via* strategies such as self-assembled monolayers, layer-by-layer deposition, or polymer entrapment, researchers have achieved improved selectivity and lower detection limits for target compounds. These CD-functionalized interfaces are further enhanced by combination with carbon nanotubes, graphene, metal nanoparticles, and redox mediators, providing synergistic effects that boost conductivity, catalysis, and signal amplification. Moreover, CD-based sensors exhibit reversible recognition, making them amenable to repeated use and continuous monitoring. Notably, derivatization of the CD ring expands its applicability, introducing functionalities such as chirality recognition, metal coordination, or improved solubility. Different detection modes, including voltammetry, impedance, and competitive displacement assays, have been reported for a variety of analytes, ranging from heavy metals and pesticides to pharmaceuticals and chiral compounds. The incorporation of CDs into advanced hybrid architectures also offers solutions to common issues like electrode fouling and limited selectivity, thus expanding their utility in harsh or complex sample environments. While challenges remain in ensuring reproducibility, large-scale manufacture, and robust performance in real-world applications, ongoing innovations in materials science and synthetic chemistry promise to make CD-based electrodes increasingly valuable for sensitive, portable, and cost-effective chemical analysis. Furthermore, novel integration with biological receptors, such as enzymes and aptamers, holds promise for multiplexed biosensing.

Received 11th April 2025
Accepted 10th May 2025

DOI: 10.1039/d5ay00612k

rsc.li/methods

Introduction

Electrochemical sensors have become indispensable tools across biomedical diagnostics and environmental monitoring, offering sensitive, selective detection with relatively low cost and portability.[1–3] A critical factor in such sensors is the incorporation of molecular recognition elements that confer selectivity towards target analytes.[4,5] Traditionally, biological receptors like enzymes, antibodies, and aptamers have been used,[6,7] but there is growing interest in synthetic supramolecular hosts such as cyclodextrins (CDs).[8] CDs are cyclic oligosaccharides known for their ability to form host–guest inclusion complexes with a wide range of molecules.[9–11] By virtue of a hydrophobic interior cavity and a hydrophilic exterior surface, CDs can encapsulate hydrophobic or appropriately sized guest molecules in water, enhancing the sensor's selectivity *via* molecular recognition.[9,12] In electrochemical sensing, this inclusion phenomenon can be leveraged to pre-concentrate targets near an electrode or to modulate electron-transfer events, enabling detection of otherwise challenging analytes.[13–15]

In recent years, CD-based architectures have garnered increasing attention for chemical sensor development.[16] These architectures integrate CDs into electrode interfaces either directly or in combination with functional materials, marrying the molecular recognition capabilities of CDs with the catalytic or conductive properties of nanomaterials and polymers.[17] Notably, CDs have been combined with carbon nanomaterials, conducting polymers, metal nanoparticles, and biological recognition elements to create hybrid sensing interfaces with synergistic performance. Such hybrids can achieve high sensitivity alongside high selectivity.[18] Diverse analytes have been targeted using CD-based sensors, ranging from metal ions and small organic pollutants to pharmaceutical compounds and biomarkers.[19,20] The results include notable enhancements in

[a]*College of Materials and Environmental Engineering, Hangzhou Dianzi University, Hangzhou, 310018, China. E-mail: hassan@uestc.edu.cn; fuli@hdu.edu.cn*
[b]*The Quzhou Affiliated Hospital of Wenzhou Medical University, Quzhou People's Hospital, Quzhou, 324000, China*

detection limits and the ability to discriminate among structural isomers or enantiomers by selective inclusion.[21] A brief timeline highlighting major milestones in the development of CD-based electrochemical sensors is presented in Fig. 1. This historical overview helps contextualize the evolution from basic host–guest studies to sophisticated hybrid architectures integrating CDs with nanomaterials, redox mediators, and biological recognition elements.

The field has matured significantly, and several valuable reviews have previously surveyed the landscape of CD-based electrochemical sensors. For instance, early work focused on the fundamental principles of CD modification. More specific reviews have detailed the application of CD-modified sensors for drug analysis[22] or summarized advances using functional composites based specifically on β-cyclodextrin.[23] Another recent review focused broadly on CDs as supramolecular recognition systems in electrochemical sensor fabrication.[24] While building upon these foundations, the present review distinguishes itself by providing a comprehensive and up-to-date perspective specifically focused on the diverse architectural strategies employed in designing CD-based sensing interfaces and, critically, the development and synergistic function of CD-based functional hybrid materials. We survey the progress from simple CD immobilization (*e.g.*, self-assembly, electropolymerization) to the rational design of sophisticated hybrid architectures where CDs are integrated with various advanced functional materials, including metal/metal oxide nanoparticles, diverse carbon nanomaterials (graphene, CNTs, nanodiamonds), conducting polymers, and metal–organic frameworks (MOFs). Our scope encompasses α-, β-, and γ-CDs and their derivatives, illustrating how their combination with these materials leads to enhanced electrocatalytic activity, improved conductivity, increased surface area, and novel recognition capabilities. Furthermore, this review synthesizes recent advancements (covering literature primarily from 2018 to early 2024) across a broad spectrum of applications, including environmental pollutant detection, pharmaceutical quality control, and clinical biomarker sensing, highlighting how these engineered CD-hybrid architectures address contemporary analytical challenges. By focusing on the design principles, material integration strategies, and synergistic effects within these complex architectures, this review aims to provide a unique and forward-looking perspective on the state-of-the-art and future directions in the field. We begin in Section 2 with the structural features of CDs and their molecular recognition properties, laying the foundation for understanding host–guest interactions. Section 3 discusses the various strategies to incorporate CDs into electrochemical interfaces - from simple adsorption and self-assembled monolayers to polymeric entrapment and electropolymerization techniques. Building on these methods, Section 4 explores hybrid architectures where CDs are integrated with functional materials (carbon nanostructures, polymers, metals, *etc.*) to achieve superior sensor performance. In Section 5, we examine the spectrum of target analytes that CD-based sensors address and the corresponding detection mechanisms, including examples of how inclusion complexes facilitate signal transduction for different analyte classes. Finally, Section 6 highlights current challenges in the field - such as stability, reproducibility, and real-sample applicability - and outlines emerging opportunities and future directions for CD-based electrochemical sensors. Throughout the review, recent peer-reviewed literature is extensively cited to illustrate key concepts and advancements in this rapidly evolving area.

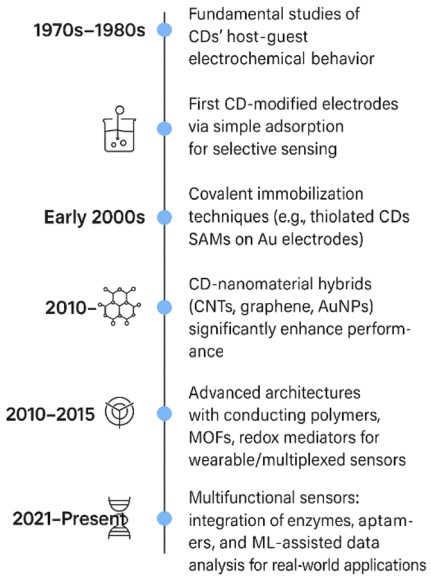

Fig. 1 Timeline of key milestones in the development of CD-based electrochemical sensing.

Structural features and recognition properties of CDs

CDs are a family of ring-shaped glucose oligomers characterized by a truncated cone (toroidal) molecular structure. The three

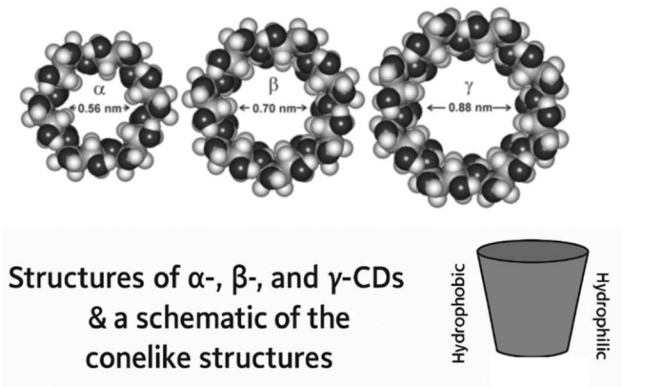

Fig. 2 Schematic representation of the molecular structures and cavity dimensions of α-, β-, and γ-CDs, each comprising 6, 7, and 8 glucopyranose units, respectively. The conelike illustrations depict their truncated cone geometry with a hydrophobic inner cavity and hydrophilic exterior, which underlies their ability to form host–guest inclusion complexes in electrochemical sensing applications.

most common native CDs – α-, β-, and γ-CDs – consist of 6, 7, and 8 glucopyranose units (Fig. 2), respectively. Owing to the chair conformation of each D-glucopyranose, the ring assumes a somewhat rigid truncated cone shape with a narrow "primary" rim (bearing C6-OH groups) and a wider "secondary" rim (bearing C2-OH and C3-OH groups). This geometry results in a hydrophilic exterior surface (all the –OH groups face outward) and a hydrophobic interior cavity lined by skeletal carbons and ether-like glycosidic oxygens. Table 1 summarizes key structural properties of the three native CDs.

The hydrophobic cavity of a CDs can accommodate guest molecules of suitable size and geometry *via* non-covalent forces.[25] CDs act as "molecular containers" or "molecular shape sorters", selectively binding guests that fit into their cavity while excluding larger molecules.[26] The driving forces for inclusion complex formation include van der Waals interactions,[27–29] hydrophobic effects, and hydrogen bonding or dipole interactions between guest and the CD's rim substituents.[30,31] Importantly, binding is reversible - the guest can enter and leave the cavity - which is advantageous for sensing applications as it allows dynamic equilibrium and signal transduction (*e.g.* guest binding or displacement can generate an electrochemical response). CDs inclusion complexes often exhibit significant molecular selectivity, preferring certain isomers or enantiomers due to the shape and functional group complementarity with the cavity environment. For example, α-CD with its smaller cavity might bind small aromatic compounds or aliphatic chains, whereas β-CD (intermediate cavity) is ideal for many pharmaceuticals and pollutants, and γ-CD can accommodate larger guests or even small peptide motifs.[32,33] Beyond size selectivity, CDs can also impart chiral recognition.[34–36] The asymmetric arrangement of hydroxyls around the CD rims means that an enantiomeric pair may bind with different orientations or affinities.[37,38] This has been exploited in sensors to distinguish D- *vs.* L-amino acids.[16,39] For instance, β-CD-based electrodes have shown differential oxidation currents for D- and L-tryptophan, effectively acting as chiral sensors.[40] The origin of this enantioselectivity lies in the three-dimensional fit of the chiral guest within the chiral CD cavity and the distinct hydrogen bonding patterns that may form with rim –OH groups.[41]

While native CDs already provide versatile binding pockets, their functionality can be further tuned *via* chemical derivatization. Each CD offers multiple hydroxyl groups that can be modified without destroying the cyclic structure.[42,43] Common derivatives include hydroxypropyl-β-CD (HP-β-CD), carboxymethyl-β-CD (CM-β-CD), amino-CDs, and thiolated CDs, among many others.[44] Such modifications can drastically alter properties: for example, adding hydrophilic groups (like hydroxypropyl) greatly increases aqueous solubility,[45,46] while introducing ionic or chelating groups (*e.g.* –COOH, $-NH_2$, –SH) provides new binding modalities or anchor points for attaching the CD to surfaces.[47,48] Table 2 highlights some representative CD derivatives relevant to electrochemical sensing. By choosing appropriate substituents, one can enhance the affinity for certain targets, incorporate redox-active moieties, or introduce functional handles for immobilization (*e.g.* thiolated β-CD for gold electrodes). Indeed, over 300 CD derivatives have been synthesized, categorized broadly as hydrophobic, hydrophilic, or ionic, each expanding the application scope of CDs in molecular recognition.[49,50]

CDs derivatives thus enable tailored molecular recognition. For instance, attaching ferrocene to a CD can create a competitive binding system where the ferrocene is hosted in a CD until a target analyte displaces it, yielding an electrochemical signal (Fig. 3).[51] Similarly, introducing charged groups can confer selectivity for oppositely charged analytes by electrostatic attraction on top of inclusion.[52] This tunability is a significant advantage of CDs: by modifying their rims, one can design hosts for specific sensing applications while preserving the underlying inclusion chemistry.

Another aspect of CD recognition in sensors is the binding strength or stability of inclusion complexes. Binding constants (K_a) for CD-guest complexes typically range from $\sim 10^2$ to 10^4 M^{-1} for many organic molecules, though stronger binding (10^5–10^6 M^{-1}) can occur for well-matched guests.[37,53,54] Such moderate binding affinities are ideal for sensor reuse and reversible signaling: the CD can capture the analyte long enough for measurement, yet the complex can dissociate upon simple washing or potential cycling to regenerate the sensor surface.[55,56] In practice, the effective selectivity and sensitivity in a CD-based sensor will depend on these binding equilibria, the kinetics of guest inclusion/release, and how the inclusion event is coupled to the electrochemical signal (*e.g.* through changes in peak current or potential). Overall, the unique structural features of CDs - their toroidal shape, hydrophobic cavity, and modifiable rims - underpin their versatile recognition properties, making them powerful building blocks for electrochemical sensing interfaces.

The binding strength between CDs and guest molecules, typically characterized by inclusion constants (K_a), plays a crucial role in determining the selectivity and sensitivity of

Table 1 Structural characteristics of α-, β-, and γ-CD. Each has a toroidal shape with a height of ~0.78 nm (7.8 Å). Cavity diameters and volumes refer to the central hydrophobic cavity. Solubility values are for water at 25 °C (approximate)

CDs	Glucose units	Molecular weight (Da)	Cavity diameter (Å)	Outer diameter (Å)	Cavity volume (nm^3)	Aqueous solubility ($g\ L^{-1}$)
α-CD	6	972.9	~4.7	~15.2	~0.53	~145 (high)
β-CD	7	1135.0	~6.0	~16.6	~0.65	~18 (low)
γ-CD	8	1297.1	~7.5	~17.7	~0.83	~249 (very high)

Table 2 Examples of modified CDs and their features

CD derivative	Modification	Notable effects on properties	Typical use in sensors
Carboxymethyl-β-CD (CM-β-CD)	$-CH_2COO^-$ groups (multiple)	Increases water solubility; introduces negative charge. Can coordinate metal cations	Attaching to amine-containing surfaces *via* amide bonding; capturing metal ions or polar guests in sensors
Hydroxypropyl-β-CD (HP-β-CD)	$-OCH_2CH(OH)CH_3$ groups	Greatly increases solubility (prevents crystallization); maintains neutral character	Enhancing dispersion of nanomaterials and biocompatibility; used in sensing of phenolics and vitamins due to high inclusion ability
Thioated β-CD (SH-β-CD)	–(CH$_2$)_*n*–SH on primary rim	Allows chemisorption to gold surfaces *via* Au–S bond; forms self-assembled monolayers. Slightly lower solubility	Creating stable CD monolayers on Au electrodes for size-selective sensing and aptamer attachment
Monoamino-β-CD (*e.g.* 6-amino-6-deoxy-β-CD)	$-NH_2$ group (single site)	Retains one primary amine for covalent coupling (*e.g.* to carboxylic surfaces) while leaving other –OH intact	Covalent immobilization on electrode coatings (*via* EDC/NHS coupling); can serve as a bridge to link CDs onto nanomaterials or polymers
Ferrocenyl-CD (*e.g.* Fc-appended β-CD)	Ferrocene appended to rim	Adds a redox-active guest or pendant to CD. Ferrocene can be included in another CD or act as a built-in mediator	Used for indicator-displacement sensing (ferrocene as signal when displaced by analyte); and as a redox probe for binding events in aptamer sensors ([CDs subject-object recognition-based aptamer sensor for sensitive and selective detection of tetracycline

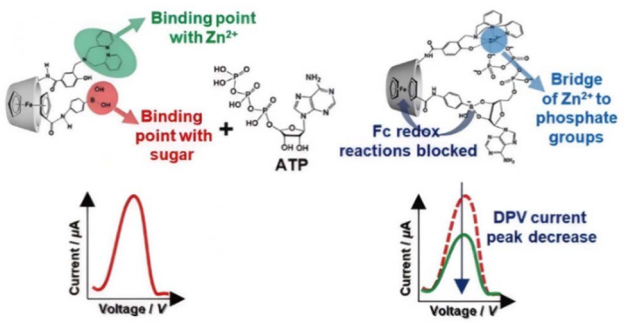

Fig. 3 The *cis*-diol binding of ribose with PBA causes a reduction of DPV current peak as the Fc redox reaction is blocked.[51]

CD-based electrochemical sensors. While K_a values in solution are well documented, evaluating these constants within sensor matrices presents additional challenges due to factors such as surface confinement effects, matrix heterogeneity, and mass transport limitations.

Several techniques have been adapted to estimate inclusion constants (K_a) in sensor environments. Electrochemical methods such as cyclic voltammetry (CV), differential pulse voltammetry (DPV), and electrochemical impedance spectroscopy (EIS) are commonly employed, as they enable the monitoring of changes in peak currents, potentials, or charge transfer resistance upon guest binding, from which apparent K_a values can be derived.[57] Isothermal titration calorimetry (ITC), although traditionally conducted in solution, has also been adapted in certain cases to study CD-guest interactions on modified surfaces, providing valuable thermodynamic information.[58] In addition, spectroscopic techniques, including fluorescence titration, UV-vis absorbance shifts, and surface plasmon resonance (SPR), allow real-time observation of inclusion events and enable quantitative determination of K_a values even under conditions where CDs are immobilized.

Despite the availability of these methods, notable discrepancies often arise between bulk solution measurements and those conducted within immobilized sensor matrices. Factors such as steric hindrance at the electrode interface, reduced accessibility of the CD cavities, and microenvironmental influences like variations in ionic strength or localized pH gradients can significantly affect the observed K_a values. These discrepancies highlight the need for careful interpretation of binding data obtained under sensor-relevant conditions.

To enhance reproducibility and enable more meaningful comparisons across different CD-based sensor systems, standardized evaluation practices have been suggested. These include performing calibration curves using both free and immobilized CDs under identical experimental conditions, employing competitive binding assays with well-characterized reference guests, and systematically reporting apparent binding constants along with detailed experimental parameters such as electrode modification strategies and the concentration ranges of the guest molecules tested. Adoption of these standardized practices would significantly contribute to the advancement of CD-based electrochemical sensing by ensuring more accurate and comparable measurements of host–guest binding interactions.

Strategies for incorporating CDs into electrochemical interfaces

Translating the molecular recognition capabilities of CDs into a functional sensor requires effective immobilization of CDs on the electrode or within the sensing interface. A variety of strategies have been developed to integrate CDs onto electrode surfaces while maintaining their host–guest functionality. Broadly, these strategies include physical adsorption or entrapment, formation of self-assembled monolayers, incorporation into polymer matrices or films, and covalent attachment either directly or *via* coupling agents. Each immobilization strategy offers distinct advantages and limitations. While drop-casting is the simplest method, it often suffers from poor mechanical stability and leaching of CDs. In contrast, self-assembled monolayers (SAMs) provide excellent stability and highly accessible CD cavities but suffer from low loading capacity. Layer-by-layer (LbL) assembly enables precise control over film thickness and composition but can be time-consuming and sensitive to ionic strength.[59–61] Polymer entrapment methods enhance mechanical robustness but risk partial blockage of CD cavities, potentially diminishing host–guest complexation efficiency. Covalent coupling methods offer the highest stability, yet they may restrict CD flexibility and inclusion efficiency due to rigid bonding configurations. Therefore, the selection of a specific immobilization method must carefully balance fabrication complexity, desired sensor robustness, and target application environment. Table 3 provides an overview of common CD immobilization methods and their key features. To provide a comprehensive overview of the different methods for integrating CDs into sensing interfaces, Fig. 4 schematically illustrates typical sensor assembly pathways, including physical adsorption, SAMs, LbL deposition, polymer entrapment, and covalent grafting.

Table 3 Common strategies for integrating CDs into electrochemical sensor interfaces

Immobilization strategy	Description and mechanism	Advantages	Considerations/challenges
Drop-casting/adsorption	CD (or CD-based complex) solution is dropped on the electrode and dried, or electrode is dipped in CD solution to physisorb a layer. The CD adheres *via* weak forces (H-bonds, van der Waals) or residue interactions.[14,62]	Simple and quick; no special chemistry required. Often used with carbon paste or screen-printed electrodes by mixing CD into the ink.[63–65]	Tends to yield loosely bound CD that can leach out. Limited stability and reproducibility; often requires a binder or matrix to hold CDs in place.[66–68]
Self-assembled monolayers (SAMs)	Thiolated or otherwise surface-reactive CDs chemisorb onto conductive substrates forming a monolayer	Forms a stable, well-defined CD layer directly on electrode. Maintains high accessibility of CD cavities at interface. Size-selective gating of electrode possible	Requires specialized CD derivatives (*e.g.* with –SH).[69] Monolayer coverage limits CD loading; multiple deposition steps may be needed for higher capacity
Layer-by-layer (LbL) assembly	Alternating layers of CD (often charged CD derivatives) and complementary polymers (oppositely charged) are deposited electrostatically.[70] Builds multilayer films incorporating CDs.[71,72]	Controlled film thickness and composition; high CD content possible in multilayer.[73] Can co-immobilize other components (enzymes, nanoparticles) within layers.[74]	Film stability depends on ionic strength (may disassemble in harsh conditions).[75,76] Diffusion through multilayers might be slower - consider film thickness.[77,78]
Polymer entrapment/ composite	CDs are embedded in a polymer matrix that is cast or electrodeposited on the electrode. *E.g.* a sol–gel or chitosan film containing CD, or electropolymerizing a CD-functional monomer.[79] Molecularly imprinted polymers (MIPs) can also include CDs as functional monomers or porogens.[80,81]	Strongly immobilizes CDs within a solid film; improves stability.[82] Electropolymerization can form uniform, adherent films with CDs covalently attached to the polymer backbone.[83] MIPs with CD can yield highly selective recognition sites.[84,85]	Potential partial blockage of CD cavities by polymer if not designed carefully. Need to ensure polymerization conditions do not destroy CD structure.[86] In MIPs, template removal must be thorough to free CD sites.[87]
Covalent coupling to surfaces	Attaching CDs *via* covalent bonds to modified electrode surfaces.[88] For instance, diazonium grafting can attach anilino-CD onto carbon surfaces.[89]	Covalent bonds prevent CD leaching, giving robust sensors. Orientations can be controlled by choosing a specific substitution site on CD for attachment (keeping other cavities free)	Multi-step surface chemistry required; risk of reducing CD inclusion ability if too many attachment points or if CD is tethered very close to surface.[88] Typically lower CD coverage compared to drop-cast or polymer methods, but higher stability

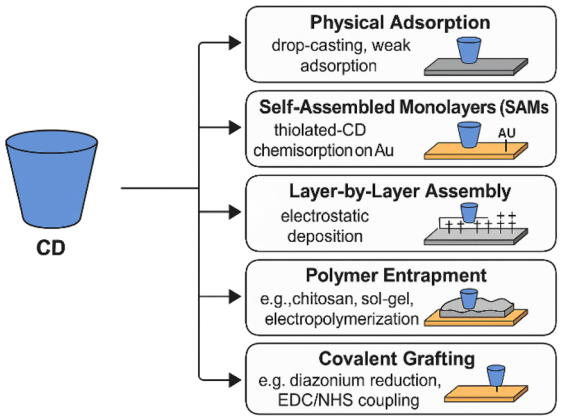

Fig. 4 Schematic overview of common sensor assembly pathways for CD-based electrochemical sensing interfaces, including physical adsorption, SAMs, LbL deposition, polymer entrapment, and covalent attachment.

Early demonstrations of CD-modified electrodes often relied on simple physical mixing or adsorption.[90,91] For example, researchers mixed β-CD powder with carbon paste or graphite inks to create screen-printed electrodes with inherent CD functionality.[92] These physically assembled systems did show the expected molecular recognition. However, a noted drawback was that CD molecules could desorb over time due to the relatively weak forces attaching them (hydrophobic and van der Waals interactions). Thus, while drop-cast and composite approaches are convenient for proof-of-concept, they often suffer from limited mechanical stability and reproducibility.[93] To address stability, researchers have increasingly turned to covalent attachment and structured films. One effective method is the formation of SAMs of thiolated CDs on gold electrodes. Thiolated β-CD (per-6-deoxy-6-mercapto-β-CD) chemisorbs onto Au *via* Au–S bonds, producing a densely packed monolayer that presents the CD cavities at the interface.[94] Such SAMs act as well-defined supramolecular interfaces: for instance, Narafu *et al.*[95] showed that ferrocene derivatives could be size-selectively included in a β-CD SAM on graphene, with electron transfer modulated by whether the ferrocene guest was bound in the monolayer or not (Fig. 5). The SAM approach yields a highly reproducible sensor surface - each CD is anchored, and the monolayer prevents aggregation or multilayer formation that might hinder accessibility. A challenge, however, is that the total loading of CD is limited to a monolayer's worth; nevertheless, this can be sufficient for sensing applications if the target analytes bind strongly.[96]

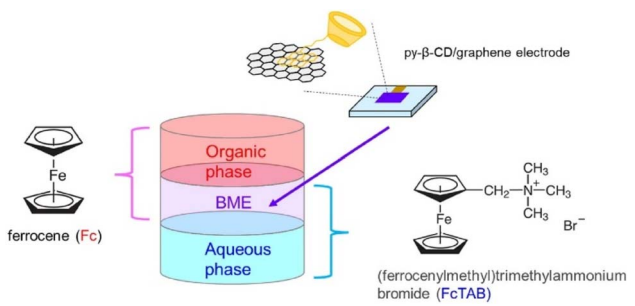

Fig. 5 Concept of Fc analysis in bicontinuous microemulsions using py-β-CD modified monolayer graphene electrode.[95]

Another robust strategy is electropolymerization of CD-containing monomers or polymers onto electrodes. In one example, Jiang *et al.*[97] electropolymerized β-CD in the presence of reduced graphene oxide to form a poly-β-CD/graphene film on a glassy carbon electrode (GCE). The resulting film was covalently grafted to the electrode and encapsulated numerous CD cavities in a conductive network, which was used to detect the antibiotic gatifloxacin with good sensitivity. Electropolymerization ensures that CDs are permanently embedded and often yields thin, uniform coatings that are advantageous for fast electron transfer. Ma *et al.*[98] similarly electropolymerized carboxymethyl-β-CD on a gold electrode (often with a nanoparticle incorporation step) to create a polymeric CD layer that improved electrocatalytic responses to biomolecules like thymine and glucose. An important consideration for polymer entrapment methods is to verify that the CD's cavity remains available - harsh polymerization conditions or dense cross-linking could occlude the cavity. Studies have shown that careful design, such as using CD derivatives with electropolymerizable groups at one site, can result in polymer backbones that hold the CD in an orientation conducive to guest binding.[99]

LbL assembly provides yet another versatile route to incorporate CDs, especially charged derivatives, into multilayer films. By alternating depositions of, say, a negatively charged CD (like CM-β-CD) and a positively charged polymer (like polycationic polyallylamine or a cationic CD derivative), one can build up films of arbitrary thickness with CDs in each layer.[100] Liu *et al.*[101] developed an electrochemical sensor for paracetamol by assembling bilayers of poly(diallyldimethylammonium chloride) (PDDA) and β-CD onto a GCE. The resulting PDDA/β-CD multilayer film enhanced electron transfer kinetics and preconcentrated paracetamol *via* host–guest interactions, achieving a detection limit as low as 0.03 μM. The CD cavities contributed to selective analyte recognition, while the LbL structure enabled fine control over film thickness and stability. In another example, Kong *et al.*[102] prepared a LbL film using chitosan (positively charged) and β-CD-functionalized carbon nanotubes (negatively charged) for dopamine detection. The incorporation of β-CD not only enhanced the molecular recognition capability toward dopamine through inclusion complexation but also improved the compactness of the CNT network, leading to lower background capacitive current and greater electrocatalytic response. These studies highlight that LbL architectures co-integrating CDs and functional materials offer a modular platform for building high-performance electrochemical sensors. The main trade-offs include extended fabrication times and the need for careful deposition control to ensure layer uniformity and reproducibility.

A more direct approach for carbon electrodes is covalent bonding *via* electrochemical grafting. One prominent technique involves diazonium chemistry: a CD derivative bearing an

aniline group (such as mono-(4-aminophenyl)amino-β-CD) can be diazotized and electrochemically reduced on a carbon surface to form a covalently bonded aryl-CD layer. Yao *et al.*[103] used this *in situ* diazonium grafting to attach mono-(*p*-aminophenyl) β-CD onto SWCNTs, producing a functional nanohybrid that enhanced detection of persistent organic pollutants. Similarly, amine-terminated CDs have been linked to carboxylated electrodes (including carbon nanotubes functionalized with –COOH) *via* amide bond formation. Alarcón-Angeles *et al.*[104] reported a GCE modified with SWCNT–COOH covalently coupled to mono-(6-hexamethylenediamine)-β-CD; the resulting CD-functionalized SWCNTs showed a remarkably low detection limit (~1 nM) for bisphenol A. The covalent route assures that the CDs remain firmly in place even under extensive usage, and by choosing mono-substituted CDs, the majority of CD cavities remain free for guest binding rather than being used up in bonding.

MIPs are synthetic materials designed to exhibit selective binding sites complementary in shape, size, and functional groups to a target molecule (template). Incorporating CDs into MIP architectures provides a powerful strategy to enhance molecular recognition capability and improve sensor performance. CDs can be integrated into MIP systems in two primary roles: (i) as functional monomers participating in the imprinting process through host–guest interactions with the template, and (ii) as porogens or pore-forming agents to tailor the MIP's morphology and facilitate mass transport. In the functional monomer approach, the cavity of the CD forms an inclusion complex with the template molecule during the polymerization, resulting in well-defined binding sites upon template removal. For example, β-cyclodextrin derivatives have been polymerized alongside conventional monomers to create recognition cavities with enhanced affinity and selectivity. This synergistic combination offers superior template binding due to the dual contribution of molecular imprinting and supramolecular inclusion. As a porogen, CDs create a highly porous MIP matrix, improving the accessibility of imprinted sites and facilitating fast analyte diffusion to the binding sites. This property is particularly beneficial in electrochemical applications where rapid response times are critical.

Hybrid architectures of CDs with functional materials

While CDs alone can impart molecular recognition to an electrode, their sensing performance is often significantly enhanced when combined with other functional materials. Different CD-based hybrid architectures offer distinct synergistic effects depending on the choice of functional material. CD-carbon nanomaterial hybrids (*e.g.*, CD-CNTs, CD-graphene) typically provide outstanding conductivity and mechanical strength but may suffer from gradual detachment if the CD attachment is not covalent. CD-–metal nanoparticle hybrids (*e.g.*, CD-AuNPs) afford significant catalytic enhancement, particularly for redox-active analytes, but often require careful size control and surface stabilization to avoid nanoparticle aggregation. CD-redox mediator hybrids offer highly sensitive displacement-based detection mechanisms but may be limited in terms of real-world stability due to mediator leaching. In comparison, CD-polymer hybrids are particularly advantageous for wearable and flexible sensors due to their mechanical flexibility and high CD loading but sometimes compromise on electron transfer rates. Thus, the rational design of CD-based hybrids should consider the trade-offs between conductivity, selectivity, fabrication scalability, and intended application specificity. As summarized in Table 4, various functional hybrids of CDs have been engineered to synergize molecular recognition with enhanced signal transduction capabilities. The following subsections detail each category with specific examples.

CDs combined with carbon nanomaterials

Carbon nanomaterials such as carbon nanotubes (CNTs), graphene, graphene oxide (GO), carbon nanohorns, and carbon quantum dots have revolutionized electrochemical sensor design due to their large surface area, excellent electrical conductivity, and chemical stability.[105,106] However, pristine carbon nanomaterials tend to aggregate in solvents and often lack inherent selectivity for analytes.[107,108] CDs provide an elegant solution to both issues: they can non-covalently functionalize carbon nanomaterials, preventing aggregation by improving dispersibility in aqueous media (thanks to CD's hydrophilic exterior), and concurrently introduce molecular recognition properties (*via* the CD cavities). The result is a CD-carbon nanohybrid that harnesses the "best of both worlds" - high surface and electronic properties from carbon and selective analyte binding from CD. A straightforward way to create CD-carbon hybrids is by physical mixing: dispersing carbon nanotubes or graphene in a CD solution. Early studies showed that simply sonicating CNTs in β-CD leads to a stable suspension, implying that CDs adsorb onto the CNT surface (likely by hydrophobic interactions along the graphitic sidewalls). Shen and Wang[109] demonstrated this by preparing a β-CD/MWCNT composite *via* dispersion in *N*,*N*-dimethylformamide; when

Table 4 Hybrid architectures of CDs with functional materials

CD-based hybrid type	Main functional partner	Benefits
CD-carbon nanomaterials	CNTs, graphene, GO, GQDs	High surface area, conductivity, improved analyte preconcentration
CD-conducting polymers	Polypyrrole, chitosan, polyaniline	Synergistic conductivity and molecular recognition
CD-metal nanoparticles	AuNPs, AgNPs, Fe_3O_4, PtNPs	Electrocatalysis, surface area enhancement, signal amplification
CD-biorecognition elements	Enzymes (GOx), aptamers	Specific biomolecular recognition, improved selectivity

deposited on an electrode, the composite allowed simultaneous voltammetric detection of guanine, adenine, and thymine - signals that were hardly observable on an unmodified electrode. The CD's presence was key to this improvement: it formed inclusion complexes with the nucleobases, effectively "trapping" them near the electrode surface to be oxidized, thereby amplifying their currents. However, one limitation noted was that the β-CD could detach from the CNTs over time because only weak forces held it there. A related approach involved using β-CD polymers (oligomeric CDs) mixed with CNTs, which slightly improved retention due to multivalent interactions but still did not ensure uniform, permanent coating.

To create more stable CD-carbon hybrids, researchers have developed methods for stronger attachment of CDs onto carbon surfaces.[110] One such method uses a π-conjugated linker: pyrene moieties have a strong affinity for graphitic carbon *via* π–π stacking.[111–113] By attaching a pyrene group to β-CD, a pyrenyl-β-CD (PyCD) can "tether" the CD onto a CNT or graphene surface firmly. Wang and Huang[114] employed this strategy to anchor β-CD on SWCNTs and detected a tetrachlorobiphenyl *via* an electrochemical impedance method. The idea was that when the tetrachlorobiphenyl guest is included in the PyCD on the CNT, it blocks electron transfer to a redox probe, thereby increasing interfacial resistance in proportion to PCB concentration. In a another work,[115] the same SWCNT/PyCD hybrid was used for direct voltammetric detection of *p*-nitrophenol. The results were impressive: the PyCD not only captured *p*-nitrophenol efficiently, but the pyrene's conjugated structure also accelerated electron transfer, yielding a high oxidation current. The sensor's sensitivity reached ∼18.7 μA μM^{-1} and the detection limit was as low as 0.86 nM for *p*-nitrophenol – a testament to the synergy of combining CD's selectivity with CNT's conductivity and the robust linking *via* pyrene. These values were far superior to those obtained with SWCNTs alone or a simple mixture of SWCNT + CD, underscoring the benefit of engineered hybrids.

Covalent functionalization is another powerful approach. In one example, diazonium chemistry (as mentioned earlier) was applied to graft an aniline-derivatized β-CD onto SWCNTs.[116,117] The product, denoted MP-β-CD/SWCNT (from mono-(*p*-aminophenyl)-β-CD), provided a stable platform for sensing several chlorinated organic pollutants; the β-CD not only improved the solubility of SWCNTs in the sensing film but also endowed it with selectivity for planar aromatic pollutants that fit the cavity.[118] Another covalent approach employed the EDC/NHS amide coupling technique to construct β-CD functionalized nitrogen-doped graphene quantum dots (NGQDs) for chiral electrochemical sensing.[119] In this method, aminated β-CD was covalently grafted onto NGQDs, which were then deposited on a GCE to produce a hybrid sensing interface. The resulting β-CD-NGQDs/GCE displayed exceptional enantioselective recognition toward tryptophan isomers. DPV revealed that the sensor showed a significantly higher peak current for L-tryptophan compared to D-tryptophan, achieving an enantiomeric recognition efficiency of 2.569. The high performance was attributed to the dual functionality of the hybrid: NGQDs enhanced conductivity and provided auxiliary interactions (hydrophobic, hydrogen bonding, and electrostatic), while β-CD selectively captured L-Trp *via* host–guest inclusion. Molecular docking simulations further confirmed this preference, showing stronger binding and more hydrogen bonds between β-CD and L-Trp than with D-Trp (see Fig. 6), thus validating the observed chiral recognition performance. Interestingly, using bridged CD dimers can further enhance binding in these hybrids. Zhao and Li[120] developed a β-CD dimer linked by a disulfide bridge, and attached it to MWCNTs (DB-β-CD/MWCNT). Because a CD dimer can engage a guest with two cavities simultaneously (cooperative binding), the hybrid exhibited superior recognition of phenolic compounds compared to single-CD hybrids. In fact, an electrode modified with the CD dimer-MWCNT detected 4-aminophenol, 4-nitrophenol, and 4-chlorophenol with higher signals and better peak separation than analogous mono-CD/MWCNT or plain MWCNT electrodes. This demonstrates that not only the combination of CD with carbon but also the architecture of the CD itself (monomer *vs.* dimer, *etc.*) can be tuned to optimize sensor response.

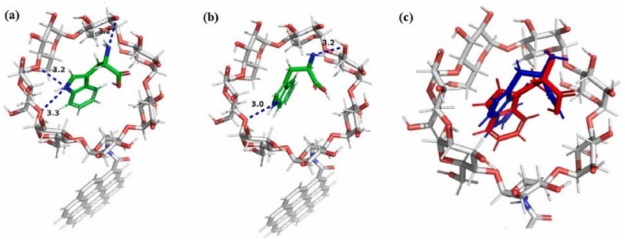

Fig. 6 (a) The binding model of β-CD-NGQDs and L-Trp. (b) The binding model of β-CD-NGQDs and D-Trp. (c) Comparison of β-CD-NGQDs and L-Trp/D-Trp binding model. (Red: L-Trp, blue: D-Trp).[119]

Beyond CNTs, CDs have also been effectively integrated with other carbon nanomaterials such as graphene and its derivatives. Owing to their planar structure and high surface area, graphene sheets are ideal for functionalization with cyclodextrins, which not only prevent their restacking *via* supramolecular interactions but also offer molecular recognition sites for analytes. A notable example is the development of a wearable electrochemical sensor based on β-CD functionalized reduced graphene oxide (β-CD/RGO) for dual pH and potassium ion detection in sweat.[121] In this system, β-CD served a dual role: it stabilized the RGO sheets in aqueous media and introduced abundant oxygen-containing functional groups, enhancing both pH sensitivity and ion-to-electron transduction capability. The β-CD/RGO composite exhibited high capacitance (∼423 μF), strong potential stability, and excellent anti-interference properties in the presence of common sweat components. For pH sensing (Fig. 7A), the β-CD/RGO-based electrode displayed a near-Nernstian slope of 54 mV dec^{-1} and a detection limit of pH 10.7. For potassium sensing (Fig. 7B), the β-CD/RGO acted as a solid-contact layer in an ion-selective electrode, achieving a Nernstian slope of 56.0 mV dec^{-1}. The flexible electrodes printed with β-CD/RGO ink also maintained reliable performance under various bending states. CDs have also been integrated with carbon nanohorns (CNHs) to form multifunctional nanohybrids for electrochemical sensing. A representative

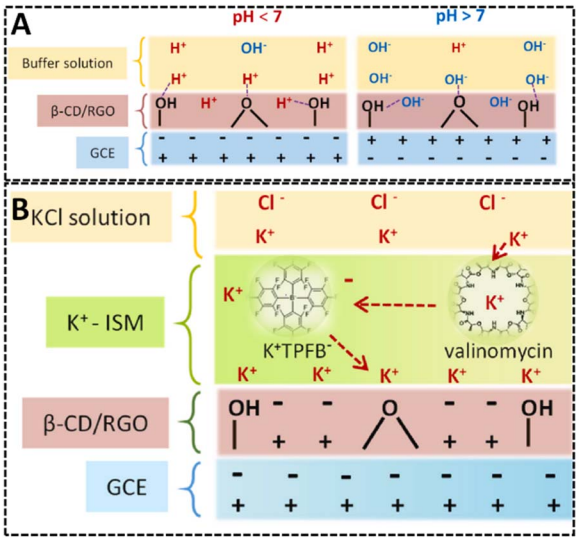

Fig. 7 (A) Representations for pH response mechanism of β-CD/RGO/GCE and (B) representations for K^+ response mechanism of K^+-ISM/β-CD/RGO/GCE.[121]

example is the MXene/CNHs/β-CD-MOFs composite,[122] which was engineered for the sensitive detection of carbendazim, a widely used but potentially hazardous fungicide. In this system, CNHs served as spacers to prevent restacking of the conductive MXene sheets, thereby increasing the electroactive surface area and enhancing ion diffusion. Simultaneously, β-CD units—embedded within a porous metal–organic framework (MOF)—provided selective molecular recognition *via* host–guest inclusion with carbendazim. This architecture allowed for high enrichment of the analyte and facilitated its electrochemical oxidation. The synergistic effects of MXene's conductivity, CNHs' structural support, and β-CD's selective binding enabled a remarkably low detection limit of 1.0 nM and a wide linear response range from 3.0 nM to 10.0 μM.

The general outcome of combining CDs with carbon nanomaterials is a multiplicative effect: the nanocarbon ensures that electron transfer for the included analyte is efficient (often electrocatalytic oxidation/reduction currents are higher), and the CD ensures that the analyte is localized and recognized.[123] A practical advantage is that many such hybrids can be prepared in a one-step mixing or co-synthesis process (*e.g.* one-pot hydrothermal synthesis of CD-graphene composites, or *in situ* reduction of GO in presence of CD[124–126]). This simplicity bodes well for scaling up sensor fabrication.[92] However, careful optimization (*e.g.* CD : CNT ratio, choice of linker) is needed to maximize the loading of CD without electrically insulating the network. The examples above illustrate that well-engineered CD-carbon hybrids can achieve extremely low detection limits for a variety of aromatic and environmental pollutants by exploiting the strengths of each component.[127]

CD-polymer and CD-redox mediator hybrids

CDs are also frequently integrated with conducting polymers such as polypyrrole to create hybrid sensing films with

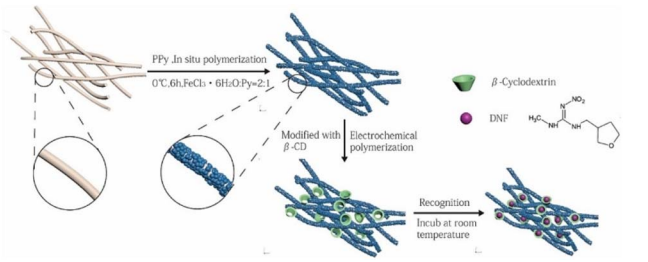

Fig. 8 Illustrates the synthesis and electrochemical detection of dinotefuran using PCL/PPy/β-CD flexible sensor.[128]

enhanced sensitivity and selectivity. These polymers can be electropolymerized or chemically deposited, forming a conductive backbone while CDs provide host–guest molecular recognition. For instance, Mei *et al.*[128] developed a flexible sensor comprising polycaprolactone (PCL), polypyrrole (PPy), and β-CD for the detection of the neonicotinoid insecticide dinotefuran (DNF). In this architecture, electrospun PCL served as a porous scaffold, PPy provided electrical conductivity, and β-CD formed a secondary porous network that enhanced electrolyte diffusion and selective DNF binding (Fig. 8). The resulting PCL/PPy/β-CD sensor achieved a low detection limit of 0.05 μM and high sensitivity of 14.07 μA μM^{-1} cm^{-2}, with excellent stability and selectivity in real rice samples. Another example comes from Palanisamy *et al.*,[129] who synthesized a GR-CD/PPy composite by chemically polymerizing pyrrole in a graphene/β-CD solution. The resulting composite was drop-cast on a screen-printed carbon electrode (SPCE) to detect trace levels of mercury(II) in water. The β-CD dispersed the graphene sheets and facilitated Hg^{2+} complexation, while PPy provided nitrogen sites for coordination and signal amplification. This sensor achieved a remarkably low detection limit of 0.47 nM for Hg^{2+}, outperforming several previous graphene- or polymer-based systems. Both examples highlight how CD-conducting polymer hybrids leverage synergistic effects–electrochemical activity from the polymer and selective molecular capture from CDs—to detect environmental contaminants with high precision.

In some designs, CDs are combined with redox mediators or labels to create a signal-amplifying hybrid. A classic concept is the competitive host–guest strategy: a redox-active guest (such as ferrocene or a ferrocene derivative) is initially included in the CD, and binding of the target analyte displaces the redox guest, altering the electrochemical signal. For example, Yang *et al.*[130] constructed a sensor where β-CD was immobilized on an electrode and 1,4-hydroquinone (HQ) was included as a redox probe; when the target cinchonine (electroinactive itself) was introduced, it displaced HQ from the CD, causing a decrease in the HQ oxidation current proportional to cinchonine concentration. Here the CD itself is the only recognition element, but the presence of a redox-active guest in the CD's cavity is critical for transduction. Such systems can be viewed as a CD-mediator hybrid (though not a chemical hybrid, more of a functional pairing) that turns binding events into current changes.

A more integrated strategy involves covalently linking a redox mediator, such as ferrocene (Fc), to CDs, enabling responsive

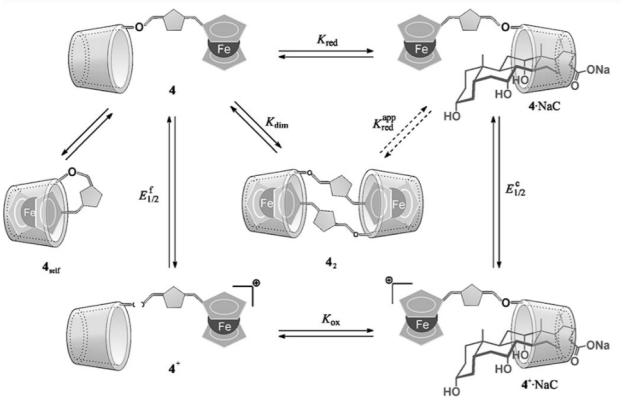

Fig. 9 Chemical and electrochemical equilibria proposed for the interaction of 4 with bile salts. The structure of complex 4^{+} ·NaC is tentative.[131]

sensing systems *via* competitive host–guest dynamics. Casas-Solvas *et al.*[131] reported the synthesis of a β-CD–ferrocene conjugate where the Fc unit is attached to the secondary face of the CD *via* a triazole linker using click chemistry. In aqueous solution, this conjugate self-assembles into a redox-controllable head-to-head homodimer, stabilized by mutual penetration of Fc units into adjacent CD cavities (Fig. 9). Notably, the electrochemical behavior of this hybrid shifts markedly upon guest binding. For example, the introduction of bile salts like sodium deoxycholate (NaDC) displaces the Fc moiety from the CD cavity, as evidenced by a cathodic shift in the half-wave oxidation potential and a rise in current intensity. This guest-induced displacement alters the local environment of Fc, enhancing its electrochemical response and supporting its utility in voltammetric sensing. The system operates *via* a CE (chemical–electrochemical) mechanism, where guest inclusion disrupts the self-inclusion equilibrium, promoting electron transfer. These hybrids demonstrate not only enhanced redox stability but also selective responsiveness, as sensitivity parameters calculated from potential shifts showed particularly high selectivity for sodium chenodeoxycholate (NaCDC) over other bile salts. Such CD–Fc conjugates thus offer a robust platform for constructing molecular sensors with tunable selectivity and improved mediator retention, effectively addressing the challenge of mediator diffusion in biosensors.

CDs with metal nanoparticles and other inorganic nanostructures

Metal nanoparticles (NPs), such as gold (AuNPs), silver (AgNPs), platinum, and metal oxides, are widely employed in sensors for their catalytic properties and high surface area. CDs can interact with metal nanoparticles in multiple ways: (i) CDs can act as capping or stabilizing agents for nanoparticle synthesis,[132] (ii) they can be attached to pre-formed nanoparticles to provide a molecular recognition layer, or (iii) they can form inclusion complexes with metal complex ions to preconcentrate them.

One promising direction in CD-gold hybrid materials involves the integration of β-CD with gold nanoparticles

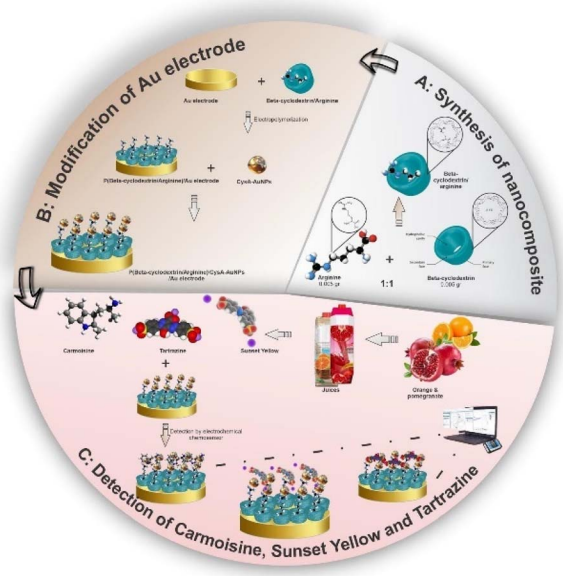

Fig. 10 Schematic illustration of the chemosensor (P(β-CD/Arg)/CysA-AuNPs/AuE) fabrication process for detection of carmoisine, sunset yellow, and tartrazine in juices.[133]

(AuNPs), yielding composites with excellent electrocatalytic and host–guest recognition properties. In one study, Luo *et al.*[133] developed an electrochemical sensor based on a GO/AuNPs/β-CD-modified glassy carbon electrode for ultra-sensitive detection of the insecticide imidacloprid. Here, β-CD enhanced selective inclusion of the hydrophobic analyte, while AuNPs and graphene oxide provided signal amplification through synergistic catalytic and conductive effects. This hybrid exhibited a broad linear range (50–3000 nM) and a low detection limit of 1.33×10^{-10} mol L^{-1}. In another example, Luo *et al.*[133] designed a multi-layered chemosensor featuring a poly(β-CD/arginine) film functionalized with cysteamine-capped AuNPs (CysA-AuNPs) for the simultaneous voltammetric recognition of synthetic dyes like carmoisine, tartrazine, and sunset yellow in juices (Fig. 10). The β-CD component served as a selective host for the dyes, while the AuNPs boosted electron transfer and signal intensity. The sensor demonstrated nanomolar sensitivity (LOQ ~1 nM) and robust selectivity in complex matrices, showing promise for food safety monitoring. A third approach by Chen *et al.*[134] involved synthesizing an HS-β-CD@Mb/AuNPs composite, where methanobactin reduced gold ions to generate AuNPs that were then stabilized and functionalized by thiolated β-CD. This structure was electrodeposited onto gold electrodes to construct a biosensor for nitrite detection. The HS-β-CD not only improved nanoparticle dispersion but also contributed supramolecular recognition, enabling rapid host–guest interactions with nitrite. This biosensor achieved a remarkably low detection limit of 0.013 μM and showed good performance in real food samples. Together, these examples underscore the versatility of β-CD/AuNP hybrids in designing sensitive and selective electrochemical sensors by exploiting both molecular recognition and nanoscale catalysis.

CDs have also been successfully incorporated into metal oxide nanostructures to enhance electrochemical sensing performance. A representative example is the MXene/Fe_3O_4/β-CD nanocomposite,[135] which was fabricated *via* self-assembly and used for the detection of guanosine 5′-monophosphate (GMP) in meat samples. In this system, β-CD played a pivotal role in selectively recognizing and enriching GMP molecules *via* host–guest interactions, while Fe_3O_4 nanoparticles offered peroxidase-like catalytic activity, and MXene provided a highly conductive matrix for electron transfer. The synergy between these components resulted in significant signal amplification. Electrochemical studies revealed a two-electron and two-proton oxidation of GMP on the composite-modified electrode, with a remarkably low detection limit of 0.0126 μM and a broad linear range from 0.05 to 600 μM. The modified electrode also demonstrated excellent selectivity against other umami substances and maintained over 92% signal stability after 15 days. This work clearly demonstrates how CD-functionalized metal oxide composites can effectively enhance sensitivity, stability, and specificity in electrochemical biosensing applications.

Another noteworthy class of CD-inorganic hybrid materials involves the integration of β-CD with MOFs, enabling highly selective and sensitive electrochemical sensing. A recent example is the β-CD/Ni-MOF/GCE composite, developed for the detection of dopamine (DA),[136] a critical neurotransmitter related to neurological disorders such as Parkinson's and schizophrenia. In this system, Ni-MOF synthesized *via* a hydrothermal route was hybridized with β-CD, forming a rough, porous surface ideal for electrochemical reactions. The β-CD provided selective binding of DA through host–guest inclusion, while the Ni-MOF facilitated electrocatalysis due to its high surface area and redox-active sites. The resulting β-CD/Ni-MOF/GCE sensor exhibited a wide linear detection range (0.7–310.2 μM) and an ultra-low detection limit of 0.227 μM. Moreover, the sensor maintained excellent reproducibility and stability, with a signal drop of less than 8% after 15 days and relative standard deviation under 6% across replicate measurements. Interference studies confirmed minimal signal distortion from common coexisting biomolecules like uric acid or glucose, demonstrating the hybrid sensor's promise in complex biological environments such as human serum. Another innovative example involves a β-CD@Ca-sacc/MeOH/GCE electrode,[137] in which β-CD is electrochemically grafted onto a calcium-saccharate-based MOF. This multichiral sensor uniquely combines two types of chiral sites: the molecular cavities of β-CD and the stereogenic backbone of the Ca-sacc/MeOH MOF. Designed for enantiomeric recognition, this hybrid platform enables simultaneous discrimination of tryptophan (Trp) and penicillamine (Pen) enantiomers with high sensitivity. DPV revealed that the hybrid sensor exhibited significant current differences between enantiomeric pairs, achieving IL/ID ratios of 2.52 for Trp and 2.08 for Pen, outperforming single-component β-CD or MOF electrodes. Detection limits reached the sub-micromolar range (*e.g.*, 0.098 μM for L-Trp), and successful analysis of racemic mixtures and rat serum confirmed the platform's analytical robustness. These examples underscore the power of combining β-CD with MOFs, offering synergistic advantages in terms of selectivity, conductivity, and signal amplification in electrochemical sensing.

Table 5 illustrates the wide range of hybrid combinations and their impressive analytical performance for environmental targets. For instance, a work shows a state-of-the-art heavy metal sensor where a film containing HP-β-CD and rGO, doped with bismuth (Bi) particles,[138] was used. Here, Bi serves as a "mercury-free amalgam" electrode material - it forms alloys with Pb and Cd during the pre-concentration step of stripping voltammetry. The role of HP-β-CD was to help create a uniform film with rGO and Nafion (a cation-exchange polymer) and possibly to bind metal complexes or keep the film hydrophilic. The detection limits achieved (sub-nanomolar for Pb^{2+}/Cd^{2+}) are among the lowest reported, showing that the combination of materials was highly effective. Notably, CDs do not strongly bind metal ions on their own (since the cavity is hydrophobic), but derivatization (like introducing carboxyls in CM-β-CD) can give some affinity for metal coordination. Even without direct binding, CDs contribute by structuring the composite film (preventing graphene aggregation, for example, as HP-β-CD does), which indirectly improves the sensor's performance.

CDs in biosensing hybrids: enzymes and aptamers

Beyond inorganic materials, CDs have been creatively combined with biological receptors to fabricate hybrid biosensors. Two notable examples are CD-enzyme and CD-aptamer hybrids.

CD-enzyme hybrids. Enzymes offer specificity through biorecognition and catalytic conversion of analytes, whereas CDs can assist in enzyme immobilization and in managing interfering substances.[143,144] A representative case is the glucose biosensor that used a CM-β-CD layer to host glucose oxidase (GOx). The carboxymethyl-β-CD not only attached GOx *via* amide bonding (forming a stable enzyme film) but also formed inclusion complexes with a ferrocene mediator, as described earlier. This multi-component assembly (enzyme + CD + mediator + conductive nanoparticles) significantly improved the sensitivity to glucose, and the CD's presence was crucial for maintaining enzyme activity by providing a friendly microenvironment (CDs are known to stabilize proteins by moderate encapsulation of hydrophobic regions.[145] Another benefit observed was that CD in the film could capture common interferents (like 4-acetamidophenol or certain drugs) that often foul glucose sensors, thereby enhancing selectivity in complex samples.[146] In essence, the CD-enzyme hybrid acted as both an immobilization matrix and a molecular sieve. Similarly, for cholesterol biosensors, β-CD has been embedded in polyaniline films with cholesterol oxidase, where CD helped trap the cholesterol substrate near the enzyme and reduced the electrode fouling by cholesterol's oxidation by-products.

CD-aptamer hybrids. Aptamers are single-stranded DNA or RNA oligonucleotides capable of recognizing specific targets with high affinity. An innovative integration strategy employs host–guest interactions between β-CD and a hydrophobic tag (*e.g.*, ferrocene) appended to the aptamer or its complement, enabling reversible docking and signal modulation. In one

Table 5 Selected examples of CD-based hybrid interfaces for environmental analytes, highlighting the synergy between CD and other functional components (LOD = limit of detection)

CD hybrid material	Target analyte	Key detection method & performance	Ref.
β-CD/AuNPs on mesoporous carbon (MC)	*p*-Nitrophenol (industrial pollutant)	DPV – LOD ~26 μM; linear range 0.1–350 μM. CD enriches nitrophenol; AuNP catalyzes its oxidation	139
α-CD/NiO NPs on rGO	*p*-Nitrophenol	Amperometry/DPV – LOD 0.12 nM; linear 1–5 μM. NiO catalyzes electro-oxidation of nitrophenol; α-CD improves selectivity	140
β-CD/graphene (exfoliated)	BSA	DPV – LOD ~13.8 nM; linear 0.125–30 μM. β-CD on graphene hosts BPA; graphene provides sensitive transduction. Used for water analysis of plastic leachates	141
β-CD + MXene/CNHs/MOF composite	Carbendazim (fungicide)	Square-wave voltammetry – LOD 1.0 nM; linear 3 nM–10 μM. Porous MOF and CNHs give high surface area; β-CD selectively binds carbendazim molecule; MXene ensures conductivity	122
β-CD/rGO with polyurethane matrix	Terbutaline (TER), nimesulide (NIM), methocarbamol (MET) - pharmaceutical pollutants	Adsorptive stripping voltammetry – LODs 0.55 μM (TER), 0.083 μM (NIM), 0.077 μM (MET). CD/rGO film in PU matrix preconcentrates the drugs; yields linear ranges in low μM. Demonstrated in spiked water samples	142
Bi^{3+}/HP-β-CD-rGO/Nafion film	Pb^{2+} and Cd^{2+} (heavy metals)	Anodic stripping voltammetry – LOD 0.09 nM (Pb^{2+}), 0.07 nM (Cd^{2+}); linear 1–90 nM. Bismuth (Bi) forms alloys with target metals for efficient stripping; HP-β-CD improves dispersion of rGO and perhaps complexes metal ions weakly to aid accumulation	138

approach, Li *et al.*[147] developed an ultra-sensitive electrochemical sensor for Hg^{2+} detection based on a β-CD-modified gold electrode and a thionine-labeled T-rich aptamer. The sensor design utilized SH-β-CD self-assembled into a monolayer with interspaces that acted as "gate channels" for $[Fe(CN)_6]^{3-/4-}$ probe diffusion. In the absence of Hg^{2+}, the aptamer remains in a duplex form, keeping the redox tag distant from the electrode, allowing probe access (Fig. 11). Upon addition of Hg^{2+}, T–Hg^{2+}–T coordination occurs, inducing aptamer folding that moves thionine over the β-CD channels, effectively blocking probe access and reducing current. This gate-controlled system amplified signal changes and achieved a detection limit as low as 5.0×10^{-15} mol L^{-1}, outperforming other reported Hg^{2+} aptasensors. In a separate study, Wu *et al.*[148] designed an electrochemical aptasensor for aflatoxin B1 (AFB1) using a β-CD polymer film electropolymerized on a gold nanoparticle-modified electrode. The detection relied on the host–guest inclusion between β-CD and ferrocene (Fc). Initially, an Fc-labeled AFB1 aptamer hybridized with Fc-cDNA, forming a double-stranded complex too bulky to fit into the β-CD cavity. Upon target recognition, the aptamer preferentially binds AFB1, releasing Fc-cDNA, which then inserts into the β-CD cavity. This inclusion boosts the electrochemical signal due to enhanced electron transfer. The aptasensor exhibited a wide detection range (0.1 pg mL^{-1} to 10 ng mL^{-1}) and a limit of detection of 0.049 pg mL^{-1} using AC impedance spectroscopy.These strategies elegantly exploit the non-covalent and reversible nature of β-CD–guest interactions. CDs serve dual roles: as docking sites for electroactive tags and as smart gates modulated by aptamer-target binding events. Such systems enable sensitive, selective, and potentially reusable sensing platforms for diverse analytes.

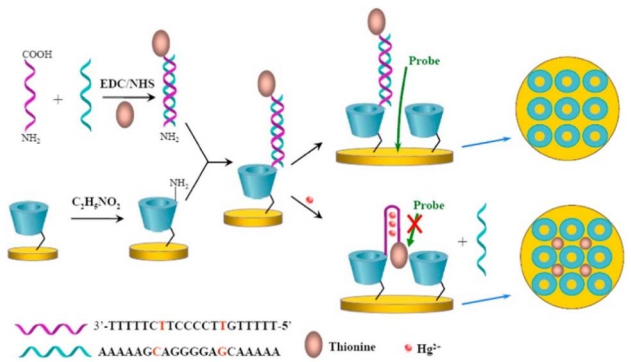

Fig. 11 Schematic of the electrochemical sensor for detecting Hg^{2+}.[147]

Target analytes and electrochemical sensing mechanisms

CD-based electrochemical sensors have been developed for a broad spectrum of analytes, including environmental contaminants (pesticides, industrial chemicals, heavy metals), food and drug residues, biomolecules (metabolites, neurotransmitters), and even chiral compounds. Table 6 summarizes the diversity of target analytes, the types of CD-based hybrid sensing architectures employed, and their typical electrochemical detection mechanisms and limits of detection. Details and representative examples are elaborated in the following sections.

Table 6 Summary of target analytes detected by CD-based hybrid electrochemical sensors

Target analyte category	Example analyte	CD-based sensing strategy	Electrochemical mechanism	Detection limit (LOD)	Ref.
Organic pollutants	*p*-Nitrophenol	β-CD/AuNPs on carbon	Direct oxidation	~26 μM	139
Pesticides	Methyl parathion	β-CD/porous carbon	Host–guest preconcentration, oxidation	5.87 nM	149
Heavy metals	Pb^{2+}, Cd^{2+}	Bi^{3+}/HP-β-CD/rGO	Anodic stripping voltammetry	~0.09 nM	138
Pharmaceuticals	Nilutamide	β-CD-AuNP/GO	Direct redox enhancement	0.4 nM	150
Biomarkers	Dopamine	β-CD/Ni-MOF	Host–guest preconcentration and catalysis	0.227 μM	136
Chiral compounds	L-/D-tryptophan	β-CD-NGQDs hybrid	Chiral differential pulse voltammetry	~μM range	119

Detection of organic pollutants and pesticides

Many organic pollutants - such as phenols, nitroaromatics, organochlorines, and azo dyes - are hydrophobic or poorly water-soluble, making them good candidates for inclusion in CD cavities.[151–154] Nitrophenols are a prime example; they are toxic and regulated pollutants often detected electrochemically by their reduction or oxidation peaks.[155–157] However, nitrophenols exist as different isomers (*ortho*, *meta*, *para*) which can be hard to distinguish.[158–160] β-CD has been used to improve the selective detection of *p*-nitrophenol (PNP) in the presence of *o*-nitrophenol by preferential binding: *p*-nitrophenol is slightly less sterically hindered and can form a more stable inclusion complex, leading to a relatively higher current for PNP oxidation on a β-CD-modified electrode. In one study,[161] an electrode coated with β-CD on fullerene could detect PNP with LOD 2.8 nM and separate its voltammetric signal from that of the o-isomer.

Organophosphate pesticides such as methyl parathion (MP) are among the most toxic and widely used insecticides, and their accurate detection is critical for ensuring environmental and food safety. CD-based hybrids have proven to be highly effective in electrochemical sensing of MP due to the host–guest recognition properties of CD and the signal amplification offered by functional nanomaterials. In one study, Fang Li *et al.*[149] developed a high-performance electrochemical sensor based on biomass-derived porous carbon spheres modified with β-CD (SJPCS@β-CD) for the rapid determination of MP in vegetables (Fig. 12). The porous carbon provided high conductivity and adsorption capacity, while β-CD promoted selective molecular recognition and dispersion. The resulting SJPCS@β-CD-modified GCE exhibited excellent performance with a linear response from 0.01–10 μM and a low detection limit of 5.87 nM. Moreover, when applied to real vegetable samples such as onions, spinach, and cabbage, the sensor demonstrated satisfactory recoveries (96.5–100.5%) and low relative standard deviations (1.06–4.25%). Another efficient design was reported by Zhou *et al.*,[162] who fabricated a β-CD/graphitized and carboxylated MWCNTs (β-CD/GR-MWCNTs-COOH) nanocomposite for MP detection. This composite leveraged the high surface area and electrical conductivity of GR-MWCNTs-COOH and the selective molecular binding ability of β-CD. The modified GCE showed a clear electrochemical response to MP through both irreversible reduction of nitro groups and a pair of reversible redox peaks related to hydroxylamine/nitroso transformations. Under optimized conditions (pH 7.0 and 120 s enrichment), this sensor achieved a low detection limit of 27 nM with a linear range from 0.01 to 15 μM. Real sample tests with spiked tap and lake water confirmed the sensor's practical utility, showing recoveries between 95.6% and 100.1% and RSDs under 4.1%.

Polyaromatic hydrocarbons (PAHs) and polychlorinated biphenyls (PCBs) are persistent, hydrophobic pollutants of significant environmental concern. CD-based architectures have been developed to enhance their electrochemical or spectroscopic detection by leveraging host–guest interactions. For instance, Chen *et al.*[163] developed a novel indirect electrochemical sensing platform for 3,3′,4,4′-polychlorinated biphenyls (PCB77) based on a β-CD-functionalized electrode. Specifically, a thiolated β-CD (β-CD-SH) was assembled with reduced GR and AuNPs on a GCE. Methylene blue (MB) was used as a redox probe, competing with PCB77 for inclusion in the CD cavity. The competitive binding of PCB77 displaced MB from the β-CD cavity, resulting in a proportional drop in MB's reduction peak current—thus enabling indirect quantification of PCB77. This sensor achieved a detection limit of 0.028 μM and demonstrated high selectivity and sensitivity, owing to both the conductivity of GR/AuNPs and the host–guest specificity of β-CD-SH. In the context of PAHs, Hahm *et al.*[164] designed a surface-enhanced Raman spectroscopy (SERS) substrate based

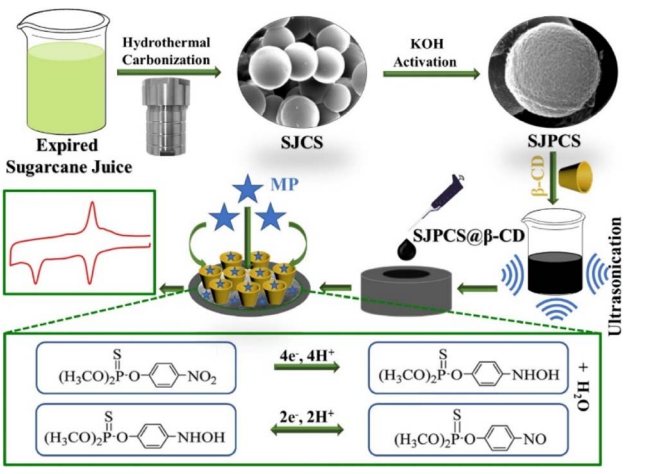

Fig. 12 Determination of MP using electrochemical sensor fabricated from β-CD (SJPCS@β-CD).[149]

on silver-embedded silica nanoparticles modified with a bridged β-CD dimer. The system, denoted as β-CD dimer@Ag@SiO_2 NPs, capitalized on the strong SERS enhancement at silver "hot spots" and the improved binding affinity of dimeric CDs. This hybrid structure enabled selective and sensitive detection of multiple PAHs, including perylene, pyrene, benzo[*a*]pyrene, and phenanthrene, by forming stable host–guest complexes. Notably, perylene could be detected down to 10^{-8} M, with distinct Raman peaks corresponding to characteristic vibrations. Furthermore, the system allowed multiplex detection of PAHs based on their unique SERS spectral fingerprints, and even maintained stability after repeated washing cycles.

Detecting metal ions like Pb^{2+}, Cd^{2+}, Cu^{2+}, and Hg^{2+} with high sensitivity often relies on electrochemical stripping techniques. CDs, being organic molecules, do not directly chelate metal ions strongly (except possibly *via* inclusion of organometallic complexes or weak dipole interactions). Nonetheless, CDs contribute to heavy metal sensing in indirect ways: by improving the morphology and stability of the electrode surface (as we saw with HP-β-CD in the Bi film for Pb/Cd), by carrying functional groups that bind metals (like thio-β-CD for Hg^{2+} binding, or CM-β-CD providing carboxyl groups that can coordinate Cu^{2+}), or by hosting hydrophobic complexes of metals. An example of the latter is detecting mercury using a "gate-controlled" CD-aptamer sensor described earlier:[147] while the aptamer provided primary recognition of Hg^{2+}, the CD's role was to transduce that binding event by holding/releasing a ferrocene.

For Cu^{2+} detection, two notable examples demonstrate the effectiveness of cyclodextrin-based hybrid materials. In the first, Chen *et al.*[165] developed an electrochemical sensor using a self-assembled Cu^{2+}-coordinated β-CD/nitrogen-doped carbon quantum dots (Cu-β-CD/N-CQDs) composite. In this design, β-CD coordinated with Cu^{2+} to form Cu-β-CD, which was then combined with nitrogen-doped CQDs *via* self-assembly. The resulting hybrid exhibited strong Cu^{2+} affinity and enhanced electrochemical performance. Differential pulse stripping voltammetry revealed a detection range of 1–125 Mm and a low detection limit of 0.094 μM, attributed to the uniform nanostructure and high dispersion of Cu-β-CD on N-CQDs. The electrode also showed high selectivity and stability in real water samples, with recovery rates between 92% and 120% and RSD values ranging from 2.3% to 5.2%. In another study, Bao *et al.*[166] fabricated a β-CD/CMK-8 nanocomposite sensor by ultrasonic blending. CMK-8 is a three-dimensional mesoporous carbon known for its high conductivity and surface area. The composite structure allowed β-CD to remain exposed on the carbon surface, enabling selective binding of Cu^{2+} *via* a binuclear hydroxyl bridge mechanism. The electrochemical sensor demonstrated a remarkably low detection limit of 0.3 ng L^{-1} and a broad linear detection range from 0.1 ng L^{-1} to 1 mg L^{-1}. Enhanced current responses were attributed to the synergistic interaction between β-CD's selective binding and CMK-8's conductivity and surface area. This sensor also performed well in real sample applications, showing excellent repeatability and reproducibility.

Detection of pharmaceuticals and drug residues

CDs are well-known in pharmaceutical sciences for their ability to form inclusion complexes with drugs, improving solubility and stability. This same property is useful in sensors for drug molecules: CDs can sequester drugs from the sample and bring them to the electrode. A notable example is the voltammetric determination of nilutamide, an anticancer drug, using a screen-printed carbon electrode modified with a β-CD-AuNP/GO composite.[150] This sensor achieved an impressive detection limit of 0.4 nM. The enhanced electrocatalytic performance stemmed from the synergistic effects of graphene oxide's conductivity, AuNP's electron transfer capability, and β-CD's selective binding. The β-CD formed stable inclusion complexes with nilutamide, effectively increasing its local concentration at the electrode surface. This composite exhibited superior peak current and lower reduction potential for nilutamide compared to control electrodes, confirming the critical role of β-CD in analyte preconcentration. Another powerful configuration is the β-CD-functionalized magnetic GO nanoparticle (β-CD-MGONP) platform coupled with a β-CD-modified carbon paste (β-CD-MCP) sensor.[167] This dual-layered sensing strategy was employed for tetracycline (TC) and doxycycline (DC) detection in milk. The β-CD-MGONPs acted as efficient extractants in a solid-phase preconcentration step, while the β-CD-MCP electrode served for DPV detection. The system achieved ultra-low detection limits of 0.18 ng L^{-1}, corresponding to ~0.4 nM. The dual use of β-CD maximized selectivity, allowing the recognition of structurally similar antibiotics through differential redox behavior. This highlights the potential of CD-based sensors not only for enhanced detection sensitivity but also for real-sample analysis in complex matrices. A third compelling case is the use of a chiral nanocomposite consisting of sulfobutyl ether-β-CD (SBE-β-CD) embedded in carbon nanofibers (CNFs) to discriminate enantiomers of amlodipine, metoprolol, and clenbuterol.[41] These pharmaceuticals exist as enantiomeric pairs with differing pharmacological effects. The SBE-β-CD nanocomposite provided a chiral microenvironment for enantioselective electrochemical recognition *via* differential pulse voltammetry. Enantiomers were distinguished based on their distinct peak potentials, with stability constant differences and Gibbs free energy shifts confirming the preferential binding. This sensor not only identified drugs at micromolar levels but also differentiated bioactive stereoisomers, underscoring the chiral selectivity endowed by CD derivatives.

Responsiveness of CD-based sensors toward disease-related biomarkers

The application of CD-based electrochemical sensors for the detection of disease-related biomarkers has received increasing attention, given the demand for highly sensitive, selective, and non-invasive diagnostic tools. CDs, by virtue of their host–guest recognition capability and ability to stabilize biorecognition elements, significantly enhance sensor performance toward clinically relevant targets.

Dopamine, a critical neurotransmitter implicated in Parkinson's disease and other neurological disorders, has been

widely targeted using CD-functionalized sensors. For example, a β-CD/Ni-MOF hybrid sensor exhibited a low detection limit of 0.227 μM and high selectivity for DA in serum samples, attributed to the synergistic effect of molecular recognition and catalytic amplification.[136]

In diabetes management, glucose biosensors incorporating CD layers, such as CM-β-CD hosting GOx, have demonstrated improved enzyme immobilization, enhanced signal stability, and resistance to common electrochemical interferents. CDs contribute by maintaining enzyme bioactivity and facilitating electron transfer, resulting in high sensitivity and long-term operational stability.

Electrochemical detection of cholesterol has also benefited from CD-polymer composite films, where CDs assist in substrate capture and reduce electrode fouling by oxidation by-products. CD inclusion complexes effectively preconcentrate cholesterol at the electrode interface, boosting sensor responsiveness. Recent studies have explored wearable CD-based sensors for non-invasive sweat analysis, targeting ions (*e.g.*, K^+) and small metabolites, thereby enabling real-time health monitoring.

Overall, the integration of CDs not only improves the affinity and selectivity toward biomarkers but also stabilizes the biorecognition interface, prolonging sensor lifespan. These attributes underscore the promise of CD-based architectures in advancing point-of-care diagnostics and personalized healthcare applications.

Detection of biomolecules in clinical analysis

CD-based sensors have proven valuable for detecting small biomolecules that often coexist and interfere with each other's detection. A classic trio in clinical diagnostics is ascorbic acid (AA), DA, and uric acid (UA).[168–170] These three species are present in blood or cerebrospinal fluid and have overlapping oxidation potentials on bare electrodes, making selective detection difficult.[171] Various CD hybrids have tackled this "ABC" problem by selectively improving the response of one or more components and/or shifting their peak potentials apart.[172]

One outstanding example is the RGO-β-CD-MWCNT-polyoxometalates (POMs) tetracomponent hybrid, which achieves remarkable simultaneous detection of AA, DA, and UA[173] The sensor exploits the high conductivity of carbon nanostructures, catalytic activity of POMs, and selective inclusion behavior of β-CD. The resulting modified GCE displayed clear, well-separated peaks for AA, DA, and UA using DPV, with detection limits of 0.84 μM, 0.04 μM, and 0.05 μM, respectively. Real sample recovery in urine ranged from 94% to 108%, demonstrating both accuracy and biocompatibility. A second representative system involved a β-CD polymer electropolymerized on rGO modified SPE (β-CD/rGO/SPE).[174] This electropolymerized sensor showed excellent peak resolution for AA, DA, and UA, benefiting from the conductive β-CD matrix and graphene's high surface area. Detection limits were 0.067 mM for AA, 0.017 μM for DA, and 0.026 μM for UA, showing comparable or better sensitivity than many multicomponent composites. Another efficient architecture utilized AuNPs integrated with β-CD-functionalized graphene (AuNP–β–CD–Gra)[175]. This sensor achieved simultaneous detection of AA, DA, and UA with detection limits of 10 μM, 0.15 μM, and 0.21 μM, respectively. The synergistic effect of AuNPs (providing catalytic sites), β-CD (improving selectivity), and graphene (facilitating electron transfer) enabled successful application in real urine samples with reliable results. Lastly, a more complex 3D hybrid consisting of reduced graphene oxide, Fe_3O_4 nanoparticles, and hydroxypropyl-β-CD (HP-β-CD)—termed 3D-rGO/Fe_3O_4/HP-β-CD—was employed for simultaneous electrochemical sensing of 5-HT, DA, and AA[176]. This nanocomposite provided separated peak potentials at −0.044 V (AA), 0.16 V (DA), and 0.316 V (5-HT), with ultra-low LODs of 3.3 nM, 6.7 nM, and 3.3 μM, respectively. Its strong catalytic activity, magnetic enrichment capability, and CD-based molecular recognition allowed efficient analysis in complex matrices like serum with recoveries above 96%.

Detection of chiral analytes

Chiral discrimination remains a critical task in pharmaceutical and biomedical sensing, as many biologically active compounds exhibit stereoselective effects. Cyclodextrins, owing to their chiral glucose-based structure and asymmetric spatial cavity, naturally impart enantioselectivity in host–guest inclusion, which can be utilized in electrochemical sensors. The primary mechanism involves differential binding affinities of enantiomers with the CD cavity, resulting in distinguishable peak shifts, current changes, or accumulation efficiencies.

A compelling example is the construction of a cross-linked metal–organic framework (CLMOF) using β-CD coordinated with potassium ions and diphenyl carbonate, yielding a stable chiral framework even in aqueous conditions[177]. When integrated with GO onto a GCE, the resulting GO-CLMOF composite exhibited significant enantiomeric recognition for mandelic acid (MA), with a peak potential difference of 96 mV and an I_L/I_D ratio of 1.8. The improved electrochemical response stems from the formation of diastereomeric host–guest complexes between the enantiomers and the CD-MOF matrix. This strategy demonstrates how structural rigidity and aqueous compatibility can be balanced for real-sample applications. Moving beyond MOFs, microporous organic networks (MONs) have been explored as an alternative CD-based platform.[178] A Sonogashira–Hagihara coupling reaction between heptakis-6-iodo-6-deoxy-β-CD and 1,4-diethynylbenzene yielded a CD-MON with abundant binding sites and a high surface area. Immobilized on a BSA-coated electrode, the resulting sensor discriminated L- and D-tryptophan with an I_L/I_D of 2.02. The synergistic interaction between CD-MON and BSA—where BSA acts both as a stabilizer and a secondary chiral selector—enabled enhanced reproducibility and specificity. This highlights the role of protein co-modification in improving the electrochemical stability and chiral resolution of CD-based sensors.

In a third approach, metal-ion modification of CDs—specifically the incorporation of Cu^{2+} into β-CD—further refined the enantioselectivity of Trp detection.[179] In one study, a multilayered electrode structure incorporating Cu^{2+}–β-CD, Au@Pt

bimetallic nanoparticles, and poly(cysteine) achieved an I_L/I_D of 2.38. The inclusion of Cu^{2+} forms hydroxy-bridged binuclear coordination at the CD cavity entrance, narrowing the effective aperture and modulating the binding orientation of enantiomers. When combined with electrocatalytically active nanomaterials, the system amplified the signal difference and enabled sensitive enantiomeric ratio analysis in serum samples. This strategy illustrates the integration of chemical coordination and nanostructured amplification in sensor design. Finally, a multicomponent sensor system comprising Cu^{2+}-modified β-CD, β-CD-based MOF, and carboxylated carbon black (CB-COOH) offered a hybrid platform for dual recognition pathways.[180] Cu–β-CD favored D-Trp *via* inner-cavity coordination, while the β-CD-MOF exhibited a stronger preference for L-Trp, collectively yielding a peak current ratio (I_L/I_D) of 2.13. This dual-host system leverages differing inclusion preferences of each selector to simultaneously accommodate both enantiomers with enhanced differential signals. The design emphasizes how combinatorial material strategies can surpass the limitations of single-host systems, yielding both sensitivity and modular selectivity.

These diverse implementations collectively reflect the versatility of cyclodextrins in chiral electrochemical sensing. Whether *via* MOF stabilization, organic network expansion, metal coordination, or dual-host assembly, the CD core serves as a reliable scaffold for tuning enantioselectivity. These findings reinforce the growing role of CD-based electrochemical platforms in high-throughput enantiomer detection, with promising implications for drug development, clinical diagnostics, and metabolomic profiling.

Challenges, opportunities, and future outlook

Despite the significant progress in integrating CDs with nanomaterials, polymers, and other functional interfaces for electrochemical sensing, several challenges must be addressed to fully harness their potential. These challenges span from fundamental scientific questions about host–guest complexation and film stability to translational barriers in reproducibility and large-scale manufacturing. Yet, opportunities abound for advancing CD-based systems into a new generation of sensors with higher performance, specificity, and real-world applicability.

One pressing challenge is stability and reproducibility in sensor construction. While CDs are readily derivatized, the precise arrangement of CD molecules on an electrode or within a composite film can significantly affect host–guest interactions and, consequently, sensor performance. Subtle variations in immobilization chemistry—such as differences in surface density, linker length, or deposition technique—can reduce reproducibility across sensor batches and hinder widespread adoption.[99,181] Ensuring robust and consistent fabrication protocols becomes crucial when transitioning from laboratory prototypes to commercial devices. A second issue is surface fouling and nonspecific adsorption, particularly when testing real samples. Proteins, organic matter, and other interferents can adsorb onto the sensor interface, blocking or competing with the CD cavities. This can diminish the sensor's ability to detect target analytes *via* host–guest inclusion. Although additional surface modification strategies (*e.g.*, blocking agents or antifouling coatings) can mitigate fouling, such protocols may add extra complexity and cost to the fabrication process.[136]

Complex binding equilibria further complicate sensor operation, particularly with multi-component or complex mixtures of analytes. Cyclodextrin-based interfaces often rely on moderate binding constants that support reversible inclusion complexes. However, in samples that contain multiple molecules competing for the CD cavity or that exhibit overlapping redox peaks, the sensor may show reduced selectivity or must be carefully calibrated to account for binding competition. A final challenge lies in scaling up both the synthesis of CD derivatives and the coupling of CDs to advanced materials (*e.g.*, graphene, carbon nanotubes, or metal nanoparticles). While cyclodextrins themselves are relatively inexpensive and can be produced in large volumes, many specialized derivatives (*e.g.*, thiolated or carboxymethyl CDs) require multi-step syntheses with moderate yields and tight reaction control. In parallel, the reproducible preparation of well-defined hybrid nanomaterials also remains nontrivial.

In spite of these hurdles, several avenues are ripe for development. First, tailored chemical functionalization of CDs holds promise for creating precisely tuned host–guest interactions. By grafting moieties that improve water solubility, binding affinity, or electrode anchoring, researchers can build sensors optimized for a particular class of analytes—whether small organic toxins or large biomacromolecules. Emerging synthetic methodologies (*e.g.*, click chemistry, modular polymerization) can streamline the assembly of advanced CD architectures with improved surface coverage and orientation. Furthermore, multifunctional sensor designs can marry CDs with other recognition elements, such as aptamers or enzymes, to expand detection capabilities. For instance, an enzyme-based biosensor might incorporate CDs to enrich a hydrophobic substrate near the electrode while the enzyme confers catalytic specificity. Similarly, aptamers can bind non-redox-active molecules, and a CD–aptamer hybrid surface may synergistically enhance overall selectivity by combining host–guest recognition with aptamer-based binding. From a materials perspective, nanostructured hybrids of CDs with carbon nanomaterials, conducting polymers, or metal–organic frameworks present a major opportunity. The high surface area and conductivity of these substrates can amplify electrochemical signals and improve the kinetics of host–guest inclusion. For example, the incorporation of CDs within graphene-based films not only stabilizes the graphene sheets (preventing restacking), but also enables selective preconcentration of analytes in the hydrophobic cavities.

Several directions for future research and technological advancement are evident. First, standardized protocols for preparing CD-based sensing interfaces, including uniform derivatization procedures and well-characterized film-deposition methods, would bolster reproducibility and scale-

up. Robust guidelines that detail surface coverage, cavity orientation, and washing/activation routines would assist both academic and industrial labs in consistently reproducing sensor performance. Second, machine learning and computational modeling could guide the design of next-generation CD architectures by predicting optimal substituents or polymer backbones for specific target molecules. Insights from molecular dynamics simulations of host–guest complexes, for example, could accelerate the discovery of novel CD derivatives with tunable binding pockets. Lastly, real-sample testing and regulatory pathways will become increasingly important as CD-based sensors move beyond the proof-of-concept stage. Demonstrating stable performance in raw biological fluids or environmental samples—where pH fluctuations, ionic strength, and complex interferent mixtures can confound detection—is key for commercial viability. In parallel, regulatory standards in clinical diagnostics or environmental monitoring will require thorough validation, from linearity and detection limits to shelf-life and robustness under storage.

Conclusion

Over the past decades, CD-based architectures have emerged as versatile and powerful tools in electrochemical sensing, displaying remarkable capabilities for selective molecular recognition, signal transduction, and enhanced stability. By exploiting the unique toroidal shape, hydrophobic cavities, and modifiable rims of CDs, researchers have engineered sensors to preconcentrate an extensive range of targets, including environmental pollutants, metal ions, pharmaceuticals, and biomolecules. Strategies for incorporating CDs into electrode interfaces, such as drop-casting, self-assembled monolayers, layer-by-layer deposition, polymer entrapment, and covalent coupling, collectively enable stable films tailored to diverse analytes and operating conditions. Equally pivotal is the synergy realized by combining CDs with functional materials—carbon nanostructures, metal nanoparticles, redox mediators, and biological recognition elements—thereby amplifying conductivity, catalytic activity, and specificity. These hybrid systems, from CD–carbon nanotube composites to CD–enzyme conjugates, demonstrate extraordinary sensitivity, low detection limits, and consistent performance even in complex matrices. Mechanistic insights reveal that host–guest inclusion in the CD cavity can facilitate direct redox processes, trigger competitive displacement events, or alter interfacial properties, culminating in quantifiable electrochemical signals. Thanks to moderate binding affinities and reversible inclusion equilibria, many CD-based sensors offer regeneration capabilities and reusability. Notable successes encompass the simultaneous detection of multiple analytes with overlapping oxidation potentials, the enantioselective discrimination of chiral molecules, and the ultratrace measurement of toxic metals. However, challenges remain, including reproducibility issues, potential surface fouling, limited understanding of complex binding equilibria, and the need for standardized, scalable synthesis of CD derivatives. Ongoing developments suggest that advanced CD modifications, such as ferrocenyl or thiolated derivatives, along with emerging hybrid strategies that integrate aptamers, enzymes, or metal–organic frameworks, can address these concerns by refining selectivity, boosting signal amplification, and stabilizing sensor interfaces. Overall, CD-based platforms stand poised to transform electrochemical sensing, offering durable, low-cost, and highly sensitive devices suitable for point-of-care testing, environmental surveillance, and industrial applications. By leveraging improvements in fabrication methods and computational design, future innovations will likely produce even more robust, multiplexed, and miniature sensors that integrate seamlessly into real-world monitoring scenarios. Moreover, the emergence of machine learning-based optimization and sophisticated computational tools promises accelerated discovery of tailored CD derivatives for specific analytes, further refining sensor performance. Significant achievements also include the rational design of hierarchical films that improve mass transport, enhance detection kinetics, and preserve CD cavities for dynamic inclusion.

Data availability

No primary research results, software or code have been included and no new data were generated or analysed as part of this review.

Author contributions

Li Fu: conceptualization, supervision, methodology, writing – original draft, project administration. Hassan Karimi-Maleh: conceptualization, methodology, writing – review & editing, project administration. Xingxing Li: investigation, formal analysis, data curation, visualization. Fei Chen: investigation, formal analysis, data curation. Yanfei Lv: investigation, data curation. Rui Zhang: investigation, data curation. Shichao Zhao: supervision, writing – review & editing.

Conflicts of interest

There are no conflicts to declare.

References

1 A. Chen and S. Chatterjee, *Chem. Soc. Rev.*, 2013, **42**, 5425–5438.
2 D. Li, S. Song and C. Fan, *Acc. Chem. Res.*, 2010, **43**, 631–641.
3 Z. Saddique, M. Faheem, A. Habib, I. UlHasan, A. Mujahid and A. Afzal, *Diagnostics*, 2023, **13**(10), 1737.
4 A. Dhaffouli, P. Salazar, S. Carinelli, M. Holzinger, B. Rodrigues and H. Barhoumi, *Chemosensors*, 2025, **13**, 87.
5 S. Fathi-Karkan, S. Sargazi, S. Shojaei, B. Farasati Far, S. Mirinejad, M. Cordani, A. Khosravi, A. Zarrabi and S. Ghavami, *Nanoscale*, 2024, **16**, 12750–12792.
6 K. Ikebukuro, C. Kiyohara and K. Sode, *Biosens. Bioelectron.*, 2005, **20**, 2168–2172.
7 J. Swensen, Y. Xiao, B. Ferguson, A. Lubin, R. Lai, A. Heeger, K. Plaxco and H. Soh, *J. Am. Chem. Soc.*, 2009, **131**, 4262–4266.

8 L. Geng, J. Sun, M. Liu, J. Huang, J. Dong, Z. Guo, Y. Guo and X. Sun, *Food Chem.*, 2024, **437**, 137933.
9 D. Prochowicz, A. Kornowicz and J. Lewiński, *Chem. Rev.*, 2017, **117**, 13461–13501.
10 Z. Liu, X. Dai, Y. Sun and Y. Liu, *Aggregate*, 2020, **1**, 31–44.
11 Y. Inoue, Y. Liu, L. Tong, B. Shen and D. Jin, *J. Am. Chem. Soc.*, 1993, **115**, 10637–10644.
12 L. Fritea, M. Tertiș, C. Cristea and R. Săndulescu, *Electroanalysis*, 2023, **35**(1), e202200014.
13 J. Liu, X. Leng, Y. Xiao, C. Hu and L. Fu, *Nanoscale*, 2015, **7**, 11922–11927.
14 H. Wu, F. Fang, C. Wang, X. Hong, D. Chen and X. Huang, *Biosensors*, 2021, **11**(7), 21610.3390/bios11070216.
15 J. Wei, X. Zhang, Q. Chang, S. Mugo and Q. Zhang, *Anal. Chem.*, 2023, **95**, 15786–15794.
16 L. Chang, Q. Li, P. Weidler, Z. Gu, C. Wöll and J. Zhang, *CCS Chem.*, 2022, **4**, 3472–3481.
17 A. Rothfuss, J. Ayala, J. Handy, C. McGranahan, K. García-Pedraza, S. Banerjee and D. Watson, *ACS Appl. Mater. Interfaces*, 2023, **15**, 39966–39979.
18 L. Rosales-Vázquez, A. Dorazco-González and V. Sánchez-Mendieta, *Dalton Trans.*, 2021, **50**, 4470–4485.
19 X. Dong, D. Li, Y. Li, H. Sakiyama, M. Muddassir, Y. Pan, D. Srivastava and A. Kumar, *CrystEngComm*, 2022, **24**, 7157–7165.
20 X. Fan, L. Jiang, Y. Liu, W. Sun, Y. Qin, L. Liao and A. Qin, *Opt. Mater.*, 2023, **137**, 113620.
21 S. Yang, S. Wu, J. Liu, H. Fa, M. Yang and C. Hou, *IEEE Sens. J.*, 2021, **22**, 2993–3000.
22 J. Lenik, *Curr. Med. Chem.*, 2017, **24**, 2359–2391.
23 X. Niu, Z. Mo, X. Yang, M. Sun, P. Zhao, Z. Li, M. Ouyang, Z. Liu, H. Gao, R. Guo and N. Liu, *Microchim. Acta*, 2018, **185**, 328.
24 B. Healy, T. Yu, D. C. da Silva Alves, C. Okeke and C. B. Breslin, *Materials*, 2021, **14**, 1668.
25 T. Urooj, M. Mishra and S. Pandey, *Discov. Environ.*, 2024, **2**, 65.
26 K. Assaf and W. Nau, *Acc. Chem. Res.*, 2023, **56**, 3451–3461.
27 S. Treccani, J. Alongi, A. Manfredi, P. Ferruti, R. Cavalli, G. Raffaini and E. Ranucci, *Polymers*, 2022, **14**(15), 2022.
28 A. Aman, S. Ali, P. Mahalapbutr, K. Krusong, P. Wolschann and T. Rungrotmongkol, *RSC Adv.*, 2023, **13**, 27244–27254.
29 G. Raffaini, S. Elli, F. Ganazzoli and M. Catauro, *Macromol. Symp.*, 2022, 2100305.
30 J. Xie, X. Li, Z. Du, Y. Liu and K. Zhu, *CCS Chem.*, 2022, **5**, 958–970.
31 C. Kouderis, S. Tsigoias, P. Siafarika and A. Kalampounias, *Molecules*, 2023, **28**(3), 1147.
32 X. Chen, H. Chen, L. Đorđević, Q. Guo, H. Wu, Y. Wang, L. Zhang, Y. Jiao, K. Cai, H. Chen, C. Stern, S. Stupp, R. Snurr, D. Shen and J. Stoddart, *J. Am. Chem. Soc.*, 2021, **143**, 9129–9139.
33 H. Dossmann, L. Fontaine, T. Weisgerber, V. Bonnet, E. Monflier, A. Ponchel and C. Przybylski, *Inorg. Chem.*, 2021, **60**, 930–943.
34 L. Chen, Y. Chen, Y. Zhang and Y. Liu, *Angew. Chem., Int. Ed. Engl.*, 2021, **60**, 7654–7658.
35 Y. Wang, Y. Sun, H. Bian, L. Zhu, D. Xia and H. Wang, *ACS Appl. Mater. Interfaces*, 2020, **12**, 45916–45928.
36 X. Wang, J. Wu, X. Liu, X. Qiu, L. Cao and Y. Ji, *ACS Appl. Mater. Interfaces*, 2022, **14**, 25928–25936.
37 H. Chai, C. Zhao, S. Wang, M. Quan, L. Yang, H. Ke and W. Jiang, *CCS Chem.*, 2020, **2**, 440–452.
38 J. Bílek, D. Koval, V. Šolínová, H. Talele, L. Severa, P. Gutiérrez, F. Teplý and V. Kašička, *J. Sep. Sci.*, 2024, **47**, e2400286.
39 D. Wu, L. Tan, C. Ma, F. Pan, W. Cai, J. Li and Y. Kong, *Anal. Chem.*, 2022, **94**, 6050–6056.
40 J. Ji, L. Qu, Z. Wang, G. Li, W. Feng and G. Yang, *Microchem. J.*, 2022, **175**, 107133.
41 P. Kalambate, S. Upadhyay, Y. Shen, W. Laiwattanapaisal and Y. Huang, *J. Materiomics*, 2020, **7**, 226–235.
42 S. Yaacob, M. Suwaibatu, R. Jamil, N. Zain, M. Raoov and F. Suah, *J. Chem. Technol. Biotechnol.*, 2022, **98**, 312–330.
43 F. Alshati, T. Alahmed, F. Sami, M. Ali, S. Majeed, S. Murtuja, M. Hasnain and M. Ansari, *Curr. Pharm. Des.*, 2023, **29**, 2853–2866.
44 G. Kali, S. Haddadzadegan and A. Bernkop-Schnürch, *Carbohydr. Polym.*, 2024, **324**, 121500.
45 X. Zhang, J. Su, X. Wang, X. Wang, R. Liu, X. Fu, Y. Li, J. Xue, X. Li, R. Zhang and X. Chu, *Molecules*, 2022, **27**(9), 2761.
46 Y. Lin, S. Hu, P. Huang, T. Lin and F. Yen, *Pharmaceutics*, 2020, **12**(6), 552.
47 X. Zhong, N. Lv, M. Zhang, Y. Tan, Q. Yuan, C. Hu, M. Ma, Y. Wu and J. Ouyang, *Crystals*, 2023, **13**, 1496.
48 V. Agarwal, V. Gupta, V. Bhardwaj, K. Singh, P. Khullar and M. Bakshi, *ACS Appl. Mater. Interfaces*, 2022, **14**, 6428–6441.
49 G. Scriba, *J. Sep. Sci.*, 2024, **47**, e2400148.
50 N. Tarannum, D. Kumar and N. Kumar, *ChemistrySelect*, 2022, **7**(22), e202200140.
51 M. Casulli, I. Taurino, T. Hashimoto, S. Carrara and T. Hayashita, *ACS Appl. Bio Mater.*, 2021, **4**, 3041–3045.
52 Y. Pan, H. Wang, X. Xu, H. Tian, H. Zhao, X. Hu, Y. Zhao, Y. Liu, G. Ding, Q. Meng, B. Ravoo, T. Zhang and D. Guo, *CCS Chem.*, 2020, **3**, 2485–2497.
53 Y. Ma, M. Quan, X. Lin, Q. Cheng, H. Yao, X. Yang, M. Li, W. Liu, L. Bai, R. Wang and W. Jiang, *CCS Chem.*, 2020, **3**, 1078–1092.
54 L. Payne, J. Josephson, R. Murphy and B. Wagner, *Molecules*, 2020, **25**(21), 4928.
55 D. Lee, W. Lee and J. Kim, *J. Am. Chem. Soc.*, 2023, **145**, 17767–17778.
56 Z. Panahi, M. Merrill and J. Halpern, *ACS Appl. Polym. Mater.*, 2020, **2**, 5086–5093.
57 J. Guo, J. Hou, J. Hu, Y. Geng, M. Li, H. Wang, J. Wang and Q. Luo, *Chem. Commun.*, 2023, **59**, 9157–9166.
58 G. Crini, *Prog. Polym. Sci.*, 2005, **30**, 38–70.
59 C. Zhang, R. Lang and X. Wen, *Alexandria Eng. J.*, 2024, **91**, 550–557.
60 X. Zhu, C. Cheng, X. Qin and Y. Wang, *J. Hazard. Mater.*, 2025, **485**, 136870.
61 B. Peng, F. Du, S. Dou, Y. Yang, M. Zhou, S. Zhao and Y. Fang, *Food Chem.*, 2025, **484**, 144361.

62 B. Martins, Y. Barbosa, C. Andrade, L. Pereira, G. Simão, C. de Oliveira, D. Correia, R. Oliveira, M. da Silva, A. Silva, N. Dantas, V. Rodrigues, R. Muñoz and R. Alves-Balvedi, *Biosensors*, 2020, **18**(8), 81.
63 A. Wong, A. Cárdenas-Riojas, A. Baena-Moncada and M. Sotomayor, *Microchem. J.*, 2021, **164**, 106032.
64 K. Pliuta and D. Snigur, *ChemistrySelect*, 2022, e202203070.
65 S. Mutić, D. Radanović, M. Vraneš, S. GadŽurić and J. Anojčić, *Analytical Methods : Advancing Methods and Applications*, 2021, vol. 13, pp. 2963–2973.
66 Z. Xie, M. Rong and M. Zhang, *ACS Appl. Mater. Interfaces*, 2021, **13**, 28737–28748.
67 V. Sok and A. Fragoso, *Appl. Sci.*, 2021, **11**, 6889.
68 S. Zhang, Y. Huang, Y. NuLi, B. Wang, J. Yang and J. Wang, *J. Phys. Chem. C*, 2020, **124**, 20712–20721.
69 L. Jicsinszky and G. Cravotto, *Molecules*, 2021, **26**(17), 5193.
70 A. Pérez-Anes, M. Gargouri, W. Laure, H. Van Den Berghe, E. Courcot, J. Sobocinski, N. Tabary, F. Chai, J. Blach, A. Addad, P. Woisel, D. Douroumis, B. Martel, N. Blanchemain and J. Lyskawa, *ACS Appl. Mater. Interfaces*, 2015, **7**, 12882–12893.
71 M. Chaudhary, M. Sela-Adler, A. Ronen and O. Nir, *npj Clean Water*, 2023, **6**, 77.
72 J. Gong, X. Han, X. Zhu and Z. Guan, *Biosens. Bioelectron.*, 2014, **61**, 379–385.
73 Y. Wang, M. Song, J. Zhao, Z. Li, T. Wang, H. Wang, H. Wang and Y. Wang, *ACS Nano*, 2024, **18**, 22334–22343.
74 C. Zheng, S. Tao and B. Yang, *CCS Chem.*, 2023, **6**, 604–622.
75 S. Sukhishvili and S. Granick, *Macromolecules*, 2001, **35**, 301–310.
76 I. Erel-Unal and S. Sukhishvili, *Macromolecules*, 2008, **41**, 3962–3970.
77 C. Picart, J. Mutterer, L. Richert, Y. Luo, G. Prestwich, P. Schaaf, J. Voegel and P. Lavalle, *Proc. Natl. Acad. Sci. U. S. A.*, 2002, **99**, 12531–12535.
78 D. Lee, R. Cohen and M. Rubner, *Langmuir*, 2005, **21**, 9651–9659.
79 Y. Hu, Z. Zhang, H. Zhang, L. Luo and S. Yao, *Talanta*, 2011, **84**, 305–313.
80 L. Qin, X. He, W. Li and Y. Zhang, *J. Chromatogr. A*, 2008, **1187**, 94–102.
81 B. Ferreira, M. Correa-Duarte, A. Marques, F. Moreira and G. Martins, *Microchem. J.*, 2024, **200**, 110345.
82 W. Kutner, H. Wu and K. Kadish, *Electroanalysis*, 1994, **6**, 934–944.
83 B. Jones and I. Fritsch, *ECS Meeting Abstracts*, 2016, vol. MA2016-01, p. 2062.
84 W. Zhang, L. Qin, X. He, W. Li and Y. Zhang, *J. Chromatogr. A*, 2009, **1216**, 4560–4567.
85 S. Piletsky, H. Andersson and I. Nicholls, *Macromolecules*, 1999, **32**, 633–636.
86 A. Celebioglu and T. Uyar, *ACS Appl. Bio Mater.*, 2023, **6**, 3798–3809.
87 S. Mamman, F. Suah, M. Raaov, F. Mehamod, S. Asman and N. Zain, *R. Soc. Open Sci.*, 2021, **8**, 201604.
88 E. Villalobos, J. Marco and C. Yáñez, *Micromachines*, 2023, 746, DOI: **10.3390/mi14040746**.
89 J. Lacroix, *ECS Meeting Abstracts*, 2015, vol. MA2015-01, p. 1896.
90 N. Vasanthi Sridharan and B. Mandal, *ACS omega*, 2022, **7**, 45469–45480.
91 H. Jindal, A. Oberoi, I. Sandhu, M. Chitkara and B. Singh, *Int. J. Energy Res.*, 2020, **45**, 5815–5826.
92 R. Liu and X. Shi, *Molecules*, 2023, 7000, DOI: **10.3390/molecules28197000**.
93 M. Dobrzyńska-Mizera, M. Knitter, D. Szymanowska, S. Mallardo, G. Santagata and M. Lorenzo, *J. Appl. Polym. Sci.*, 2022, 52177, DOI: **10.1002/app.52177**.
94 W. Li, G. Jin, H. Chen and J. Kong, *Talanta*, 2009, **78**, 717–722.
95 S. Narafu, Y. Takashima, O. Niwa, T. Yajima and Y. Ueno, *J. Electroanal. Chem.*, 2022, **920**, 116575.
96 R. Benters, C. Niemeyer and D. Wöhrle, *Chembiochem : A European Journal of Chemical Biology*, 2001, vol. 2, pp. 686–694.
97 Z. Jiang, G. Li and M. Zhang, *Sens. Actuators, B*, 2016, **228**, 59–65.
98 Y. Hui, X. Ma, F. Qu, F. Chen, J. Yu and Y. Gao, *J. Solid State Electrochem.*, 2016, **20**, 1377–1389.
99 X. Niu, Z. Mo, X. Yang, M. Sun, P. Zhao, Z. Li, M. Ouyang, Z. Liu, H. Gao, R. Guo and N. Liu, *Microchim. Acta*, 2018, **185**, 328.
100 P. Chen, X. Wang, D. Yan and X. Hu, *Int. J. Polym. Sci.*, 2015, **2015**, 1–9.
101 Y. Liu, R. Yang, M. Zhao, H. Guo, Y. Liu, H. Yan and Z. Liu, *Int. J. Electrochem. Sci.*, 2024, **19**, 100878.
102 B. Kong, J. Zeng, G. Luo, S. Luo, W. Wei and J. Li, *Bioelectrochemistry*, 2009, **74**, 289–294.
103 J. Yao, Z. Yan, J. Ji, W. Wu, C. Yang, M. Nishijima, G. Fukuhara, T. Mori and Y. Inoue, *J. Am. Chem. Soc.*, 2014, **136**, 6916–6919.
104 G. Alarcón-Angeles, B. Pérez-López, M. Palomar-Pardave, M. T. Ramírez-Silva, S. Alegret and A. Merkoçi, *Carbon*, 2008, **46**, 898–906.
105 R. Kour, S. Arya, S. Young, V. Gupta, P. Bandhoria and A. Khosla, *J. Electrochem. Soc.*, 2020, **167**, 037555.
106 T. Yuwen, D. Shu, H. Zou, X. Yang, S. Wang, S. Zhang, Q. Liu, X. Wang, G. Wang, Y. Zhang and G. Zang, *J. Nanobiotechnol.*, 2023, **21**, 320.
107 Y. Liu, J. Ren, Y. Wang, X. Zhu, X. Guan, Z. Wang, Y. Zhou, L. Zhu, S. Qiu, S. Xiao and Q. Fang, *CCS Chem.*, 2022, **5**, 2033–2045.
108 G. Jin, H. Zhu, Y. Yang, Y. Xie, G. Wang, J. Huang, L. Shi, O. Schmidt and S. Yu, *CCS Chem.*, 2020, **2**, 1–12.
109 Q. Shen and X. Wang, *J. Electroanal. Chem.*, 2009, **632**, 149–153.
110 M. Webber and P. Dankers, *Macromol. Biosci.*, 2019, **19**, e1800452.
111 S. Affès, A. Stamatelou, X. Fontrodona, A. Kabadou, C. Viñas, F. Teixidor and I. Romero, *ACS Appl. Mater. Interfaces*, 2024, **16**, 507–519.
112 S. Fang, N. Li, T. Zheng, Y. Fu, X. Song, T. Zhang, S. Li, B. Wang, X. Zhang and G. Liu, *Polymers*, 2018, **10**(6), 610.

113 L. Jin, S. Thanneeru, D. Cintron and J. He, *ChemCatChem*, 2020, **12**, 5932–5937.
114 L. Kong, J. Wang, F. Meng, X. Chen, Z. Jin, M. Li, J. Liu and X.-J. Huang, *J. Mater. Chem.*, 2011, **21**, 11109–11115.
115 Y. Wei, L.-T. Kong, R. Yang, L. Wang, J.-H. Liu and X.-J. Huang, *Langmuir*, 2011, **27**, 10295–10301.
116 Q. Li, Y. Xu, A. Pedersen, M. Wang, M. Zhang, J. Feng, H. Luo, M. Titirici and C. Jones, *Adv. Funct. Mater.*, 2024, 2311086, DOI: 10.1002/adfm.202311086.
117 J. Nova-Fernández, D. González-Muñoz, G. Pascual-Coca, M. Cattelan, S. Agnoli, R. Pérez-Ruíz, J. Alemán, S. Cabrera and M. Blanco, *Adv. Funct. Mater.*, 2020, 2313102, DOI: 10.1002/adfm.202313102.
118 C. Dyke and J. Tour, *J. Phys. Chem. A*, 2004, **108**, 11151–11159.
119 F. Chen, H. Pei, Q. Jia, W. Guo, X. Zhang, R. Guo, N. Liu and Z. Mo, *Mater. Chem. Phys.*, 2021, **273**, 125086.
120 Y. Wei, L.-T. Kong, R. Yang, L. Wang, J.-H. Liu and X.-J. Huang, *Chem. Commun.*, 2011, **47**, 5340–5342.
121 X. Cui, Y. Bao, T. Han, Z. Liu, Y. Ma and Z. Sun, *Talanta*, 2022, **245**, 123481.
122 X. Tu, F. Gao, X. Ma, J. Zou, Y. Yu, M. Li, F. Qu, X. Huang and L. Lu, *J. Hazard. Mater.*, 2020, **396**, 122776.
123 A. Abbaspour and A. Noori, *Analyst*, 2008, **133**, 1664–1672.
124 Y. Guo, S. Guo, J. Ren, Y. Zhai, S. Dong and E. Wang, *ACS Nano*, 2010, **4**, 4001–4010.
125 W. Zhang, Z. Zheng, L. Lin, X. Zhang, M. Bae, J. Lee, J. Xie, G. Diao, H. Im, Y. Piao and H. Pang, *Adv. Sci.*, 2023, **10**, e2304062.
126 L. Fan, C. Luo, M. Sun and H. Qiu, *J. Mater. Chem.*, 2012, **22**, 24577.
127 E. Prabakaran and K. Pillay, *Nanoarchitectonics*, 2021, 61–87.
128 X. Mei, X. Wang, W. Huang, J. Zhu, K. Liu, X. Wang, W. Cai and R. He, *Food Chem.*, 2024, **434**, 137194.
129 S. Palanisamy, K. Thangavelu, S.-M. Chen, V. Velusamy, M.-H. Chang, T.-W. Chen, F. M. A. Al-Hemaid, M. A. Ali and S. K. Ramaraj, *Sens. Actuators, B*, 2017, **243**, 888–894.
130 Y. Yang, X. Yang, H.-F. Yang, Z.-M. Liu, Y.-L. Liu, G.-L. Shen and R.-Q. Yu, *Anal. Chim. Acta*, 2005, **528**, 135–142.
131 J. M. Casas-Solvas, E. Ortiz-Salmerón, I. Fernández, L. García-Fuentes, F. Santoyo-González and A. Vargas-Berenguel, *Chem. - Eur. J.*, 2009, **15**, 8146–8162.
132 A. Gupta, S. Briffa, S. Swingler, H. Gibson, V. Kannappan, G. Adamus, M. Kowalczuk, C. Martin and I. Radecka, *Biomacromolecules*, 2020, **21**, 1802–1811.
133 J. Luo, S. Li, Y. Wu, C. Pang, X. Ma, M. Wang, C. Zhang, X. Zhi and B. Li, *Microchem. J.*, 2022, **183**, 107979.
134 L. Chen, J. Song, L. Wang, X. Hao, H. Zhang, X. Li and J. Wu, *J. Solid State Electrochem.*, 2024, **28**, 305–316.
135 Y. Shi, Z. Niu, S. Chen, S. Wang, L. Yang and Y. Wang, *Food Bioprocess Technol.*, 2025, **18**, 807–817.
136 C. Chen, J. Ren, P. Zhao, J. Zhang, Y. Hu and J. Fei, *Microchem. J.*, 2023, **194**, 109328.
137 Y. Hou, J. Liang, X. Kuang and R. Kuang, *Carbohydr. Polym.*, 2022, **290**, 119474.
138 M. Lv, X. Wang, J. Li, X. Yang, C. Zhang, J. Yang and H. Hu, *Electrochim. Acta*, 2013, **108**, 412–420.
139 Y. Zhou, J. Zhao, S. Li, M. Guo and Z. Fan, *Analyst*, 2019, **144**, 4400–4406.
140 U. Solaem Akond, K. Barman, A. Mahanta and Sk. Jasimuddin, *Electroanalysis*, 2021, **33**, 900–908.
141 S. Kubendhiran, R. Sakthivel, S.-M. Chen, B. Mutharani and T.-W. Chen, *Anal. Chem.*, 2018, **90**, 6283–6291.
142 A. Wong, A. M. Santos, M. Baccarin, É. T. G. Cavalheiro and O. Fatibello-Filho, *Mater. Sci. Eng., C*, 2019, **99**, 1415–1423.
143 S. Dhiman, B. Srivastava, G. Singh, M. Khatri and S. Arya, *Int. J. Biol. Macromol.*, 2020, **156**, 1347–1358.
144 B. Srivastava, H. Singh, M. Khatri, G. Singh and S. Arya, *Int. J. Biol. Macromol.*, 2020, **165**, 1099–1110.
145 F. Biedermann, W. Nau and H. Schneider, *Angew. Chem., Int. Ed. Engl.*, 2014, **53**, 11158–11171.
146 H. Bu, A. English and S. Mikkelsen, *Anal. Chem.*, 1996, **68**, 3951–3957.
147 J. Li, M. Sun, X. Wei, L. Zhang and Y. Zhang, *Biosens. Bioelectron.:X*, 2015, **74**, 423–426.
148 S. S. Wu, M. Wei, W. Wei, Y. Liu and S. Liu, *Biosens. Bioelectron.: X*, 2019, **129**, 58–63.
149 F. Li, R. Liu, V. Dubovyk, Q. Ran, H. Zhao and S. Komarneni, *Food Chem.*, 2022, **384**, 132643.
150 R. Karthik, N. Karikalan, S.-M. Chen, P. Gnanaprakasam and C. Karuppiah, *Microchim. Acta*, 2017, **184**, 507–514.
151 R. Chalasani and S. Vasudevan, *ACS Nano*, 2013, **7**, 4093–4104.
152 J. Hu, D. Shao, C. Chen, G. Sheng, J. Li, X. Wang and M. Nagatsu, *J. Phys. Chem. B*, 2010, **114**, 6779–6785.
153 K. Bao, A. Zhang, Y. Cao and L. Xu, *Separations*, 2024, **11**, 143.
154 M. Lindsey, G. Xu, J. Lu and M. Tarr, *Sci. Total Environ.*, 2003, **307**, 215–229.
155 S. Hira, N. Muthuchamy and K. Park, *Sens. Actuators, B*, 2019, **298**, 126861.
156 A. Cardoso Juarez, E. Ivan Ocampo Lopez, M. Kesarla and N. Bogireddy, *ACS omega*, 2024, **9**, 33335–33350.
157 S. Lawaniya, G. Pandey, Y. Yu and K. Awasthi, *Nanoscale*, 2024, **16**, 13915–13924.
158 J. Wang, C. Liu, Z. Di, J. Huang, H. Wei, M. Guo, X. Yu, N. Li, J. Zhao and B. Cheng, *Chemosphere*, 2024, **367**, 143654.
159 P. Silva, B. Gasparini, H. Magosso and A. Spinelli, *J. Hazard. Mater.*, 2014, **273**, 70–77.
160 H. Zhou, S. Li, Y. Wu, D. Chen, Y. Li, F. Zheng and H. Yu, *Sens. Actuators, B*, 2016, **237**, 487–494.
161 J. A. Rather, P. Debnath and K. De Wael, *Electroanalysis*, 2013, **25**, 2145–2150.
162 Y. Zhou, T. Wu, H. Zhang, M. Zhao, Y. Shen, G. Zhu, M. Guo, Y. Liu, F. Li and H. Zhao, *Int. J. Electrochem. Sci.*, 2022, **17**, 220653.
163 W. Chen, Y. Jiang, J. Jiang, L. Qian and W. Gu, *J. Electrochem. Soc.*, 2019, **166**, B908.
164 E. Hahm, D. Jeong, M. G. Cha, J. M. Choi, X.-H. Pham, H.-M. Kim, H. Kim, Y.-S. Lee, D. H. Jeong, S. Jung and B.-H. Jun, *Sci. Rep.*, 2016, **6**, 26082.

165 J. Chen, S. Han, H. Li, X. Niu and K. Wang, *J. Electrochem. Soc.*, 2022, **169**, 117508.
166 C. Bao, Y. Lu, J. Liu, Y. Gao, L. Lu and S. Liu, *Molecules*, 2022, **27**, 4954.
167 A. A. Yakout and D. Abd El-Hady, *RSC Adv.*, 2016, **6**, 41675–41686.
168 F. Kamal Eddin and Y. Wing Fen, *Sensors*, 2020, 1039, DOI: **10.3390/s20041039**.
169 M. Mahanthappa, V. Duraisamy, P. Arumugam and S. Kumar, *ACS Appl. Nano Mater.*, 2022, **5**, 18417–18426.
170 J. Yang, J. Strickler and S. Gunasekaran, *Nanoscale*, 2012, **4**, 4594–4602.
171 R. Goyal, V. Gupta, N. Bachheti and R. Sharma, *Electroanalysis*, 2008, **20**, 757–764.
172 X. Shi, Y. Ruan, H. Wang, W. Zhao, J. Xu and H. Chen, *CCS Chem.*, 2020, **3**, 2359–2367.
173 C. Ma, P. Xu, H. Chen, J. Cui, M. Guo and J. Zhao, *Microchem. J.*, 2022, **180**, 107533.
174 X. Tian, C. Cheng, H. Yuan, J. Du, D. Xiao, S. Xie and M. M. F. Choi, *Talanta*, 2012, **93**, 79–85.
175 Q. Qin, X. Bai and Z. Hua, *J. Electroanal. Chem.*, 2016, **782**, 50–58.
176 W. Liang, Y. Rong, L. Fan, C. Zhang, W. Dong, J. Li, J. Niu, C. Yang, S. Shuang, C. Dong and W.-Y. Wong, *Microchim. Acta*, 2019, **186**, 751.
177 X. Sun, Z. Fu, M. Zhang, H. Fu, C. Lin, J. Kuang, H. Zhang and P. Hu, *Microchem. J.*, 2022, **183**, 108074.
178 X. Zhang, F. Wang and Z. Chen, *Anal. Chim. Acta*, 2024, **1316**, 342879.
179 T. Li, Y. Wang and X. Kan, *J. Electroanal. Chem.*, 2021, **902**, 115817.
180 J. Liang, Y. Song, Y. Zhao, Y. Gao, J. Hou and G. Yang, *Microchim. Acta*, 2023, **190**, 433.
181 G. Zhu, Y. Yi and J. Chen, *TrAC, Trends Anal. Chem.*, 2016, **80**, 232–241.